ISTANBUL TECHNICAL UNIVERSITY ★ ENERGY INSTITUTE

IDENTIFICATION OF THERMAL CHARACTERISTICS OF TRADITIONAL RUSSIAN STOVE BASED ON COMPUTATIONAL FLUID DYNAMICS AND ENERGY PERFORMANCE ANALYSES

M.Sc. THESIS

Hale Tuğçin KIRANT

Energy Science and Technology Division

Energy Science and Technology Programme

Thesis Advisor: Assoc. Prof. Dr. Hatice SÖZER

JUNE 2018

ISTANBUL TECHNICAL UNIVERSITY ★ ENERGY INSTITUTE

IDENTIFICATION OF THERMAL CHARACTERISTICS OF TRADITIONAL RUSSIAN STOVE BASED ON COMPUTATIONAL FLUID DYNAMICS AND ENERGY PERFORMANCE ANALYSES

M.Sc. THESIS

Hale Tuğçin KIRANT

Energy Science and Technology Division

Energy Science and Technology Programme

Thesis Advisor: Assoc. Prof. Dr. Hatice SÖZER

JUNE 2018

İSTANBUL TEKNİK ÜNİVERSİTESİ ★ ENERJİ ENSTİTÜSÜ

GELENEKSEL RUS ŞÖMİNESİNİN ISIL ÖZELİKLERİNİN HESAPLAMALI AKIŞKANLAR DİNAMİĞİ VE ENERJİ PERFORMANS ANALİZLERİ İLE İNCELENMESİ

YÜKSEK LİSANS TEZİ

Hale Tuğçin KIRANT
301151011

Enerji Bilim ve Teknoloji Anabilim Dalı

Enerji Bilim ve Teknoloji Programı

Tez Danışmanı: Doç. Dr. Hatice SÖZER

HAZİRAN 2018

Hale Tuğçin KIRANT, a M.Sc. student of ITU Institute of Energy, 301151011, successfully defended the thesis/dissertation entitled "IDENTIFICATION OF THERMAL CHARACTERISTIC OF TRADITIONAL RUSSIAN STOVE BASED ON COMPUTATIONAL FLUID DYNAMICS AND ENERGY PERFORMANCE ANALYSES", which she prepared after fulfilling the requirements specified in the associated legislations, before the jury whose signatures are below.

Thesis Advisor :	**Assoc. Prof. Dr. Hatice SÖZER** Istanbul Technical University	.....
Jury Members :	**Prof. Dr. Üner ÇOLAK** Istanbul Technical University	.....
	Dr. Lecturer Barış YILMAZ Marmara University	.....

Date of Submission : 04 May 2018
Date of Defense : 08 June 2018

To my wonderful family,

FOREWORD

I would like to thank my supervisor Assoc. Prof. Dr. Hatice SÖZER for her support and curiosity in my research. She always created opportunities to widen my knowledge since I knew her. Without her guidance and positive criticism, I would not be motivated enough to have enthusiasm on my researches.

I would like to thank to Dr. Lecturer Barış YILMAZ for his continuous encouragement since my bachelor degree. With his positive attitude, I have learnt to go forward step by step.

I would like to thank Dr. Seifu BEKELE for his valuable suggestions and supports in my thesis.

Finally, I would love to thank my wonderful family for their endless support over my career. I am so grateful for their patience and encouragements during the tough times in my research.

June 2018

Hale Tuğçin KIRANT
(Mechanical Engineer)

TABLE OF CONTENTS

Page

ABBREVIATIONS

ASHRAE	**:** American Society of Heating, Refrigerating and Air-Conditioning Engineers
CFD	**:** Computational Fluid Dynamics
FEA	**:** Finite Element Analysis
MEP	**:** Mechanical Electrical Plumbing
PMV	**:** Predicted Mean Vote
PPD	**:** Predicted Percentage Dissatisfied

SYMBOLS

C	**:** Calorific value per kg
C_p	**:** Constant pressure specific heat
D	**:** Density of the wood
E	**:** Efficiency factor
g_x	**:** Gravitational acceleration in x directions
g_y	**:** Gravitational acceleration in y directions
g_z	**:** Gravitational acceeration in z directions
h	**:** Enthalpy
k	**:** Thermal conductivity
k_E	**:** Turbulent kinematic energy
P	**:** Density of the flow
p	**:** Pressure
T	**:** Temperature
t	**:** Time
u	**:** Velocity component in x direction
V	**:** Usable volume of the stove
v	**:** Velocity component in y direction
w	**:** Velocity component in z direction
x	**:** Characteristic length
u_∞	**:** Velocity of the flow
μ	**:** Dynamic viscosity
q_V	**:** Volumetric heat source
μ	**:** Viscosity
ρ	**:** Density
ν	**:** Viscosity
σ_k	**:** Model constant
ε	**:** Dissipation rate

LIST OF TABLES

Page

LIST OF FIGURES

Page

IDENTIFICATION OF THERMAL CHARACTERISTICS OF TRADITIONAL RUSSIAN STOVE BASED ON COMPUTATIONAL FLUID DYNAMICS AND ENERGY PERFORMANCE ANALYSES

SUMMARY

The energy utilization increases day by day based on the increment of population. The new technologies focus on finding the efficient ways on energy usage to reduce the energy consumption.

The energy consumption of the residential sector occupies 25% of the total energy consumption all over the world. Likewise, the space heating consumption is the major consumption component in the residential sectors of cold climates. These circumstances indicate the necessity of the research to improve the energy performance of the heating systems.

In this study, energy performance of a traditional heating system, Russian stove, is examined based on its unique architectural detailing and energy performance. Russian stove is a commonly used heating system in Kars region where it is located at the east side of Turkey.

This study is divided in two steps as computational fluid dynamics and energy performance analysis to evaluate the performance of the Russian stove. Furthermore, a comparative analysis between Russian stove and conventional chimney with a steel casting stove were done.

A meticulous investigations were performed on applied materials and architectural design of the chimneys. The main material of the Russian stove is firestone, however, the steel casting is used in the case of contemporary stove. Addition to the applied material analysis, the chimney design of the stoves were specifically analyzed. Russian chimney has a labyrinth path design while the steel casting stove has a straight path.

The uniqueness of the chimney is arisen by its S shaped flue path, as mentioned above. S shaped flue path lets the heated air move slowly through the outlet of the chimney. Therefore, heated air, which is like 450°C, stays at the inside of the stove for a longer period by achieving a better heat transfer. Furthermore, S shaped design creates more internal surface area rather than straight chimney design that this design provides a better heat transfer with increased transfer surface area.

In this research, the original design of Russian stove was investigated in terms of energy efficiency and thermal comfort. Hence, computational fluid dynamic Software was used to evaluate the generated heat flux, thermal gradient and predicted mean vote by transient solution mode in a two story building. The evaluation was performed for both heating and standby period, separately. Besides, the thermal mass characteristic of the stoves were assessed to show the features of the used material.

In computational fluid dynamics analysis, Low Re k-epsilon turbulence model was used. Also, Petrov-Galerkin solution method, which uses second order differential

equations, was chosen. Thus, the natural ventilation and occurred secondary flows in the stove were examined. Addition to the computational fluid dynamic analysis, the heating demand of the building was simulated by energy performance simulation software and the results were compared in this purpose.

The mesh enhancement study was performed to provide the accuracy on the results. The mesh enhancements were repeated until the mesh independency was obtained at the level of 5%.

The analyses showed that, in the case of straight chimney steel casting stove, an overheating formation was observed after 3 hours and the temperature was found as 29.87°C after 6 hours heating period. Also, overheating affected the predicted mean vote as 2.71, negatively during the heating period. On the standby period, the temperature reduced significantly to 16.50°C in 6 hours and the predicted mean vote value was -1.4.

In the case of Russian stove, a homogenous heating was formed in the building and by the result of homogeneous heating, the predicted mean vote was obtained 0.3 in the heating period. Addition to this, it was observed that the generated temperature gradient was kept for 6 hours during the standby period in the building and the predicted mean vote was found as -1.

In the comparison of Russian stove and steel casting stove results, the generated heat flux was found more in the Russian stove case stove by 22%

In the conclusion of these results, in the case of Russian stove it is seen that the used material creates a thermal mass based on the high specific heat value and the unique S shape design of the Russian stove has a major effect on the thermal comfort.

The existing literature of the Russian stove was limited only by hand workmanship information. However, this research extended it to the scientific knowledge by identifying the major specifications of the system's thermal performance. The research was utilized the energy performance and computational fluid dynamics analyses. Consequently, it is shown that this system is an example of a collaborative work between architecture, material science and engineering disciplines to obtain a high performance heating system. The integration of this system to the apartment building that has multiple residential units can be studied as the next step of this research.

GELENEKSEL RUS ŞÖMİNESİNİN ISIL ÖZELİKLERİNİN HESAPLAMALI AKIŞKANLAR DİNAMİĞİ VE ENERJİ PERFORMANS ANALİZ YÖNTEMLERİ İLE İNCELENMESİ

ÖZET

Nüfusun ve tüketim toplum anlayışının artmasına bağlı olarak enerji kullanımı günden güne artış göstermektedir. Enerji tüketimini azaltmak ve enerji kullanımında verimli yöntemler geliştirmek için yeni teknolojiler üzerinde çalışmalar sürdürülmekte ve bu çalışmalar için önemli kuruluşlar tarafından destekler sağlanmaktadır.

Tüm Dünyadaki enerji tüketiminin % 25'i konut sektörüne aittir ve bu tüketimin çoğu konut ısıtma ihtiyacından kaynaklanmaktadır. Avrupa bu konu üzerinde yoğunlaşarak 2012 yılı itibariyle, 2020 yılına kadar enerji tüketiminde % 20 azalma hedefi koymuştur ve bununla ilgili bazı yönetmelikler hazırlamıştır. Ayrıca, 2030 yılına kadar enerji tüketimindeki azalmanın % 27 oranına ulaşılması gerektiği de ikinci bir hedef olarak belirlenmiştir.

Enerji verimliliği çalışmalarının yanında, kullanılan yakıtların da fosil yakıttan yenilenebilir yakıt türüne geçişi bu stratejiler arasında belirlenmiştir. Isıtma sistemlerindeki kaynak kullanımı incelendiği zaman gaz tüketiminin % 28'lik bir orana sahipken, yenilenebilir & atık kaynak kullanımının % 14 oranında olduğu görülmektedir. En çok tercih edilen yenilenebilir & atık kaynak kullanımında odunun neredeyse % 50'lik bir orana sahip olduğu ve bu oranın yıllar içinde artmakta olduğu gözlemlenmektedir.

Günümüzde enerji performans çalışmaları son teknolojiler üzerine yoğunlaşarak geçmişte kullanılan sistemlerin incelenmesi açısından zayıf kalmaktadır. Geliştirilen yeni teknolojilerin ise enerji verimli olmasının yanında, ısıl konfor şartlarını insan tabiatına uygun olarak gerçekleştirilmesi konusunda bazı eksiklikler taşıdığı görülmektedir. Isıtma-soğutma sistemlerinin kullanıcı kontrolü dışında olması, kullanılan malzemelerin insan sağlığına uyumlu olmaması ve enerji kaynağı olarak çevreyi kirleten fosil yakıtların kullanılması bu alanda yapılan çalışmalarda bazı yetersizliklerin devam ettiğini ve enerji verimliliği konusunda yeni stratejiler geliştirilmesi gerektiğini göstermektedir.

Bu stratejiler, elde edilmesi gereken ana hedefin enerji verimliliği olmasının yanında ısıl konforun ve çevresel etkilerin de enerji performansı kriterleri arasında değerlendirilmesini sağlamalıdır. Bu etmenlere bağlı olarak, birçok çalışma disiplinin birlikte yürütülmesi ile ortaya çıkmış olan eski ısıtma sistemlerinin günümüz imkânlarıyla incelenmesi hedeflenmiştir.

Bu çalışmada geleneksel bir ısıtma sistemi olan Rus şöminesinin enerji performans çalışması, enerji verimliliği ve özgün mimari yapısı incelenerek düz bacalı döküm şömine ile karşılaştırmalı olarak değerlendirilmiştir. Rus şöminesi, Türkiye'nin doğusunda özellikle Kars'ta yoğun olarak kullanılan bir geleneksel ısıtma sistemidir. Bu geleneksel ısıtma sisteminin başlıca özelliği orijinal baca tasarımından ve

yapımında kullanılan ateş tuğlası malzemesinden gelmektedir. Buna bağlı olarak, enerji performansı değerlendirmesinde bu iki parametre üzerinde yoğunlaşılmıştır.

Bacanın özgün özelliği S şeklindeki ya da labirent yoluna benzetilebilecek olan gaz akış yolundan kaynaklanmaktadır. S şeklindeki bu hava akış yolu, ısıtılmış gazın, bacanın ağzına doğru hareketini yavaşlatılmış olarak gerçekleşmesini sağlar. Bu yavaşlatılmış hareket yaklaşık olarak 450°C'ye ulaşan gazın daha fazla ısı transferi yapmasını sağlar. Ayrıca, S şeklinde gaz akış yolu, ısı transferinin gerçekleştiği iç yüzey alanına da arttırarak enerji performansına etki etmektedir. Yapımda kullanılan ateş tuğlasının bu sistemdeki avantajı ise yüksek ısıl kapasite değerinden kaynaklanıyor olup, termal kütle özelliği göstermesidir.

Düz bacalı döküm şöminenin karşılaştırmalı analiz için tercih edilmesi, kullanıcılar tarafından yoğun olarak kullanılmasına bağlı olarak gerçekleştirilmiştir. Ayrıca, çalışma sistemi Rus şöminesi ile çok benzer olduğu için karşılaştırmanın objektifliği sağlanmıştır.

Bu çalışmada yukarıda bahsedilmiş olan tasarımın özgünlüğü enerji verimliliği ve ısıl konfor perspektifinden incelenmiştir. Bu incelemede üç farklı program kullanılmıştır. İncelenecek olan binanın ve şöminelerin 3 boyutlu modellemesi yapılmıştır. Yaratılmış olan model hesaplamalı akışkanlar dinamiği programına ve enerji performans simülasyon programına aktarılmıştır. Bu programların kendi içinde uyumlu yazılıma sahip olması, oluşturulmuş olan 3 boyutlu modelin her üç programda da kullanımında kolaylık sağlamıştır.

İncelenmiş olan bina ortasında galeri bulunan, kat yüksekliği 2.7 metre olan iki katlı konut tipli bir yapıdır ve 80 m^2'lik alan üzerine oturmuş olarak toplamda 160 m^2 alana sahiptir. İncelenen şömine sistemleri binanın orta kısmına oturtulmuştur ve baca galeriden geçerek çatıya ulaşmaktadır.

Hesaplamalı akışkanlar dinamiği programı ile meydana gelen ısı akışının, ısıl gradyanın ve ortalama ısıl duyumun değerlendirmesi yukarı anlatılmış olan bina için gerçek zamanlı analizle gerçekleştirilmiştir. Bu değerlendirme ısıtma ve soğutma süreçleri için ayrı ayrı yapılmıştır. Böylece sistemin termal kütle özelliği de incelenmiştir.

Hesaplamalı akışkanlar dinamiği analizinde Low Re k-epsilon türbülans modeli kullanılmıştır. Low Re k-epsilon türbülans modeli, doğal havalandırmayı ve şömine içinde gerçekleşen ikincil akışların analizlerinde gerçeğe daha yakın sonuçlar verdiği için tercih edilmiştir

Türbülans modeline ek olarak hesaplamaların duyarlılıkla gerçekleştirilmesi için Petrov-Galerkin çözüm metot kullanılmıştır. Petrov-Galerkin çözüm metodu ikinci dereceden diferansiyel denklemlere bağlı olarak geliştirilmiş bir metottur ve sonuçlarda daha hassas veriler sağlamaktadır.

Hesaplamalı akışkanlar dinamiği analizlerine ek olarak, incelenilen binanın ısı ihtiyacı enerji performans simülasyon programı ile elde edilmiş, hesaplamalı akışkanlar dinamiği analizlerinde elde edilen sonuçlarla karşılaştırılmıştır. Bu kapsamda şömineden ısı transferinin gerçekleştiği her yüzey alanı ısıl akış hesaplarında dahil edilmiştir. Elde edilen ısıl akış sonuçları, enerji performans simülasyon sonuçlarından gelen bina ısıl ihtiyacı ile karşılaştırılmıştır. Böyle bu sistemin binanın ısıl ihtiyacına uygunluğu değerlendirilmiştir.

Enerji performans simülasyon programı, enerji simülasyonlarını gerçekleştirirken ısıl konforun elde edilmesini temel alır ve bu kapsamda American Society of Heating, Refrigerating and Air-Conditioning Engineers (ASHRAE) tarafından oluşturulmuş olan ASHRAE 55 -Thermal Environmental Conditions for Human Occupancy standardından faydalanır. Bu standartta belirtilmiş olan değerlere bağlı kalarak termal konforun sağlanması için gerekli olan güç ve enerji tüketimini hesaplar.

Isıl ihtiyaç hesaplamasında en önemli girdiler bina elemanlarının termal özellikleridir. Bu kapsamda, Türk Standartları Enstitüsü tarafından geliştirilen TS 825 - Binalarda Isı Yalıtım Kurallarından faydalanılmıştır. Bu standart, Türkiye'de gözlemlenen farklı iklimsel özelliklere bağlı olarak dört adet farklı bölge yaratmıştır. Bu bölgeler sıcak bölgeden soğuk bölgeye doğru gruplandırılmış ve her bina elemanı için uygun ısıl geçirgenlik katsayısı belirlenmiştir. Buna bağlı olarak, hem hesaplamalı akışkanlar dinamiği analizinde hem de enerji simülasyonunda biraz daha iyileştirilmiş değerler olan dış duvar için 0.36 $W/m^2.K$, pencere için 1.8 $W/m^2.K$, çatı için 0.21 $W/m^2.K$ ve taban döşemesi için 0.26 $W/m^2.K$ değeri girilmiştir. Bu değerler ile dış hava sıcaklığına bağlı olarak bina yapı elemanlarından gerçekleşen ısı transferi programda bir yıl boyunca dinamik olarak hesaplanmıştır.

Hesaplamalı akışkanlar dinamiği analizlerinde simülasyonlar, tüm model üzerinde ağ yapısı oluşturularak sağlanmaktadır. Ağ yapısının iyi oluşturulması, bilgisayar üzerinde yapılan analizlerin gerçek ortamdaki sonuçların elde edilmesi açısından önemlidir. Bu çalışmada tetrahedral ve pyramid eleman tipi kullanarak ağ yapısı oluşturulmuştur. Kullanılmış olan her iki eleman tipinin de serbestlik derecesi laminer akışlarda 5, türbülans akışlarda 7'dir.

Çözüm sonuçlarının hassaslığının sağlanması açısından ağ yapısı iyileştirme çalışması analizin önemli aşamasından birini oluşturmaktadır. Bu kapsamda ağ yapısı iyileştirme çalışmaları sonuç farklılığında %5 elde edilene kadar tekrarlanmıştır. Her iyileştirmede eleman sayılarının ve oluşmuş olan ağ noktalarının artmasından dolayı simülasyon sürelerinde artışlar görülmüştür.

Düz bacalı döküm şöminenin sonuçları incelendiği zaman ısınma süreci boyunca aşırı ısınma gözlemlendiği ve ortalama ısıl duyum değerinin 2.71 olduğu görülmüştür. Soğuma sürecinde ise sıcaklığın 6 saat içinde 16.39°C'ye düştüğü gözlemlenmiştir.

Rus şöminesi sonuçlarında ise, ısı akışının düz bacalı döküm şömineye göre % 22 oranla daha fazla olduğu bulunmuştur. Buna ek olarak, Rus şöminesinin ateş tuğlasının spesifik ısıl değerinden kaynaklanan termal kütle özelliğine bağlı olarak bina içinde homojen bir ısıl dağılım oluştuğu görülmüştür. Ortalama ısıl duyum değeri, ısıtma süreci boyunca 0.5 olarak elde edilmiştir. Ayrıca, oluşan ısıl gradiyent 6 saat boyunca soğuma esnasında da korunmuş olup ve ortalama ısıl duyum değeri -0.3 olarak bulunmuştur.

Sonuç olarak görülmüştür ki Rus şöminesinin S şeklindeki özgün baca tasarımının ısıl konfor üzerinde önemli bir etkisi olmakla birlikte kullanılan ateş tuğlası malzemesinin bina içinde termal kütle oluşturmuş olduğudur. Ayrıca, bu çalışmayla birlikte literatürde sadece el işçiliği yapımı ile kısıtlanan kaynaklar Rus şöminesinin bilimsel olarak incelenmesi ile genişletilmiştir ve ısıtma sistemlerindeki verimliliğin mimari disiplin, malzeme bilimi disiplini ve mühendislik disiplinlerinin ortak çalışması nasıl geliştirildiği ve ortaya çıkartıldığı görülmüştür. Bu çalışmanın bir sonraki aşaması olarak Rus şöminesinin, günümüzün çok katlı ve içinde konut dairesi bulunduran binalara entegrasyonu incelenebilecek seviyeye getirilmiştir.

1. INTRODUCTION

Energy utilization increases along with population rise, industrial growth and consumption habits. As the energy need increases day by day, authorities focus on energy efficiency solutions. Foundations, corporations and research institutes create funds to increase the awareness of energy efficiency and find new methods to decrease the energy consumption.

Energy consumption is initiated by different sectors such as industry, residential, transport, services and agriculture. The statistical results reveals out that the residential sector has the second greatest rate as 26% in the overall consumption throughout Europe. This consumption is caused from the space heating mostly within the total consumption by end- use that it is equal to 65%.

Different type of fuel sources such as oil, natural gas, wood are used to generate energy. The investigations show that total final consumption by fuel is reached to nearly 10000 Mtoe in 2014 and it has been increasing year by year, considerably. OECD countries have the most proportion on this consumption with 35% (Key World Energy Statistics, 2016).

Utilization of the gas and the renewables & waste have a significant place on the space heating consumption that the gas usage is 37 % while the renewables & waste usage is 16 %. The usage amount of the renewables & waste is targeted to be increased in the next years to reduce greenhouse gas emissions and the dependency on the fossil fuel.

The high rate of energy consumption and increasing fuel consumption indicate the importance of the extreme progress on the energy efficiency research. Therefore, a traditional heating system, wood burning Russian stove was examined in this study based on its material and the unique chimney design which provide energy efficient performance. The energy efficiency was evaluated by energy performance analysis and computational fluid dynamics study (CFD).

1.1 Purpose of Thesis

The sun is the basic heating source, accordingly, the fire is the second source as it takes the advantage of the radiation as sun (Grondzik et al., 2010). Fire has a significant place in the cold climate countries. It is used for lighting, cooking and heating. However, an open fire causes so much loss and doesn't provide required heating level to satisfy human thermal comfort.

This study investigates the existing strategies of energy efficiency for space heating performance evaluation by a developing analysis improved methodology. This methodology consists of the energy performance and CFD study. The purpose of this research is to investigate the traditional heating system based on its thermal characteristics . There are various researches on building energy performance to examine the efficient ways of space heating, however the most of them keep the thermal indoor comfort conditions out of scope while searching the efficient approaches on energy consumption.

The results of this study create a different point of view on modern residential heating system and builds a new line of vision on traditional heating systems. Furthermore, this study shapes a new perspective on the energy efficient buildings projects supported by European Union and United States.

The integration of building heating systems with precisely detailed architectural design has significant effects on energy consumption reduction where traditional architecture represents many impressive examples. In this context, the energy performance of traditional heating system was evaluated based on its architectural design, material characteristics and location that the stove was placed in the middle of a two-story height's galleria of a duplex house.

The Russian masonry stove is a traditional heating system, which is widely used in the city called Kars, located North East region of Turkey. The uniqueness of the heating system is expressively caused by the originality of the chimney's design whilst also functions as part of the stove. Contrast to the ordinary stoves, a labyrinth chimney model is seen in Russian masonry stoves. Furthermore, the main material of masonry stove, which is firestone, creates a significant difference with its heat capacity and conductivity value. In ordinary stoves, steel casting is used in the stove body. The

specific heat value of the steel casting is lower than the firestone's specific heat value and this feature causes a distinct difference on the energy performance of the stove.

In this principle, Russian masonry stove was examined by real time analysis that shows the occurred thermal gradient and the thermal comfort level in the space. CFD was used to present labyrinth chimney model and to show the generated heat flux. Furthermore, the heating capacity of Russian masonry stove type was compared to straight chimney ordinary stove. So, the heat flux of these two different type of stove models was observed, periodically.

1.2 Literature Review

1.2.1 The world energy utilization

The world's energy need is inclined to rise based on the population growing and the development of global economy. The energy studies show that the world primary energy demand consumption will increase as 32% between 2010 and 2035 (OECD, 2012). Energy efficiency policies and regulations are strictly in consideration by the governments and the municipalities based on the mentioned energy demand. Therefore, The 2012 Energy Efficiency Directive has provided a methodology to obtain 20% energy efficiency target by 2020 in Europe (European Energy Agency, 2015). This energy efficiency target is specified as 27% by 2030 and the increment for the share of renewables are aimed to 27% (U.S. Department of Energy, 2008); (European Commission, 2014). The existing situation on the energy consumption shows us the transport and the residential sector take up more than 50% of the total consumption.

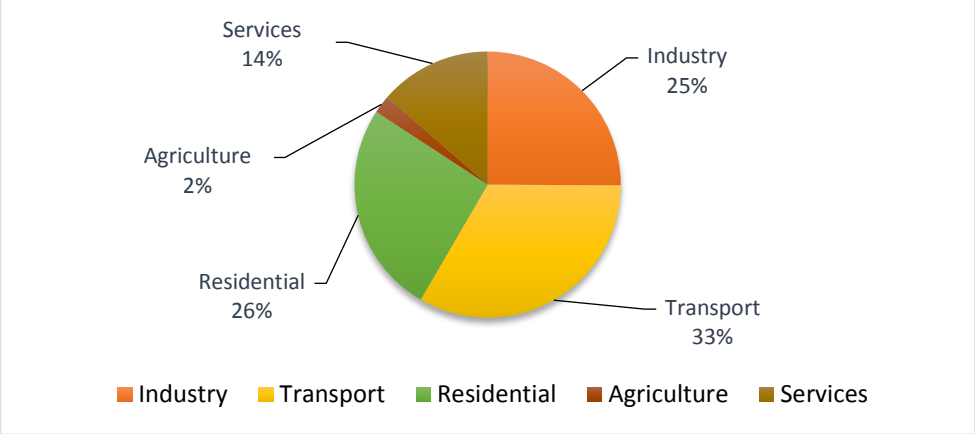

Figure 1.1 : Sectorial shares of EU-28 energy consumption (Eurostat, 2016)

The contribution of renewable sources are proposed to be included more in the next years while the increase rate of the oil and coal are intended to be reduced.

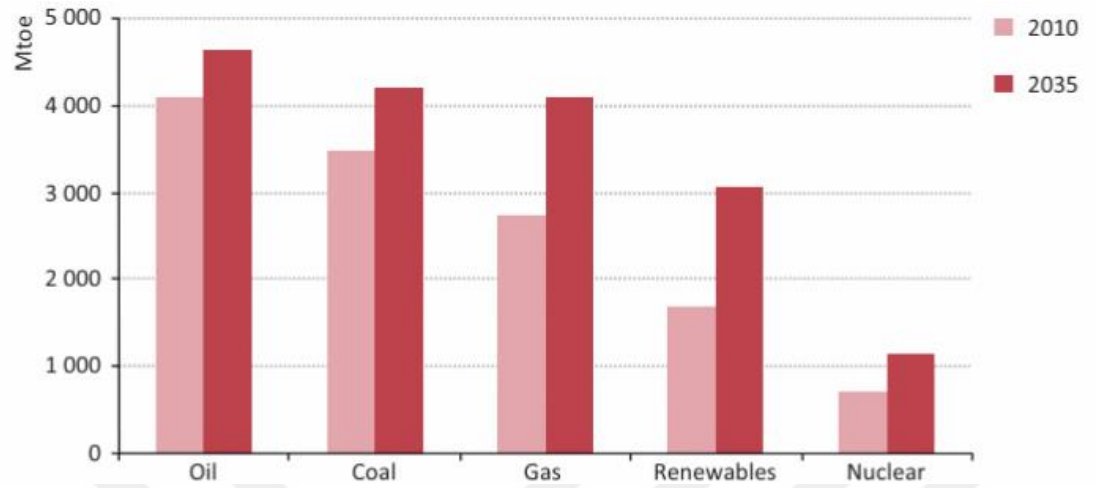

Figure 1.2 : World primary energy demand by fuel in the new policies scenario (OECD, 2012).

1.2.2 The energy utilization on space heating

The efficient systems are required to meet the overall energy demand in the residential buildings while providing energy saving. According to Eurostat statistics, space heating energy consumption is the most in the overall energy consumption for residential buildings (Url-1).

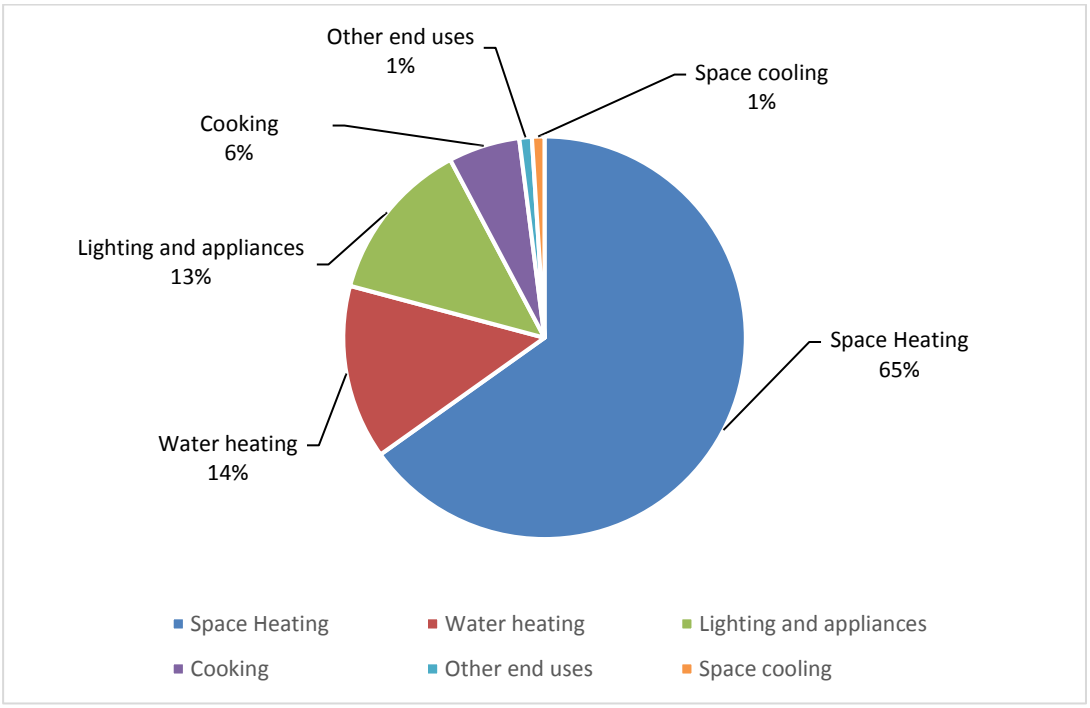

Figure 1.3 : Final energy consumption in the residential sector by type of end-use, EU-28, 2015 (Eurostat, 2018).

Thus, it shows that efficiency for space heating is more important to obtain the 2020 targets. Space heating can be generated in many ways regarding to heating systems, distribution systems and fuel types.

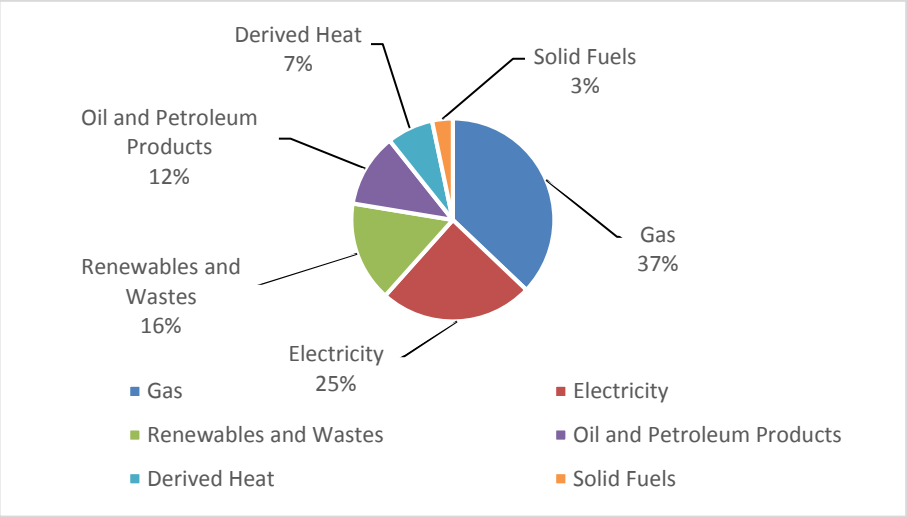

Figure 1.4 : Final energy consumption in the residential sector by fuel, EU-28, 2016 (Url-1).

Apart from the often operated heating systems, other systems are needed to be examined within detail. Stoves are one of these systems that preferred less than other conventional systems. Wood, coal or bio-ethanol are some of the used fuel types to procure combustion in stoves, however the wood is the most preferred fuel type for stoves. The characteristic feature of wood is its net calorific value (NFC). The NFC of the wood changes from 14.3 MJ/kg to 7.0 MJ/kg based on its water content (Eurostat, 2013).

1.2.3 The wood utilization as a resource

Wood is a kind of solid biofuels and it is used as fuel in the heat production and electricity generation (Eurostat, 2013). Primary production of energy from wood & other solid biofuels increases year by year that it reached to 94.1 Mtoe from 40.6 Mtoe during 1990-2016 period (Url-1). As seen in the figure 1.5, the amount of wood & other solid fuels occupies nearly 50% of the total renewable energy production (Sturc, 2012). Furthermore, the wood and its waste have a place with 5% contribution in gross inland energy consumption in the EU 27 that it has the most percentage in the renewable energy sources. In the countries which are under effect of cold climate, wood usage attains 27% of the total energy (Eurostat, 2012).

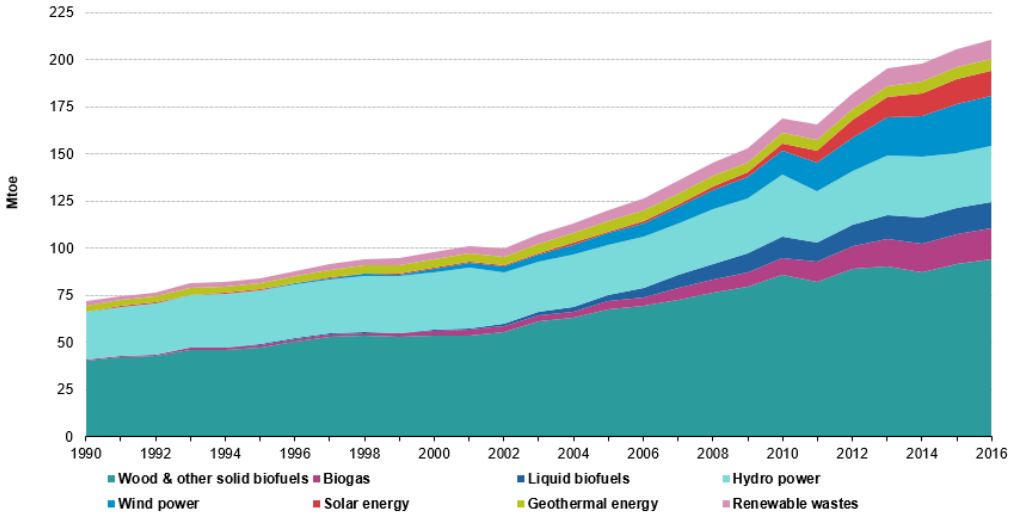

Figure 1.5 : Primary production of energy from renewable sources, EU, 1990-2016 **(**Url-1).

The most common wood heating equipment is the wood burning stove. If there is enough space, it can be installed safely in the buildings. The center of the entrance floor is the most appropriate place to install the wood burning stove. This type of installation provides the required performance level with the least maintenance (Canada Mortgage and Housing Corporation, 2002).

1.2.4 Categorization of the wood stoves

There are many types of wood burning stove designs that they differ from culture to culture. Regional climate conditions change the used material of the stoves based on the geographical sources. Addition to this, architectural concept of the regions designates the general model of the stoves.

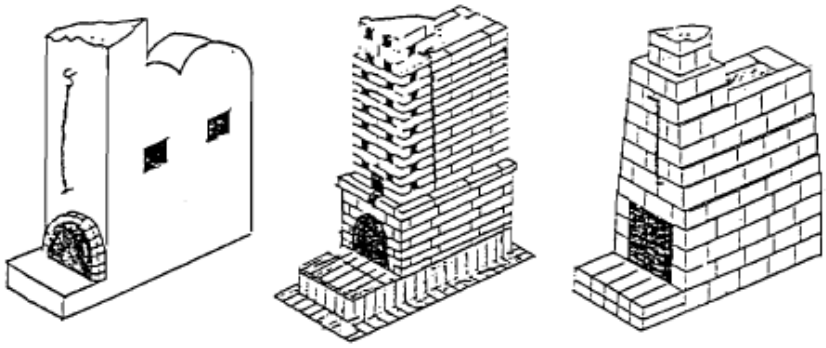

Willard Santa Fe Roswell

Figure 1.6 : Several types of designed masonry stove from Willard, Santa Fe and Roswell (Missouri Department of Natural Resources).

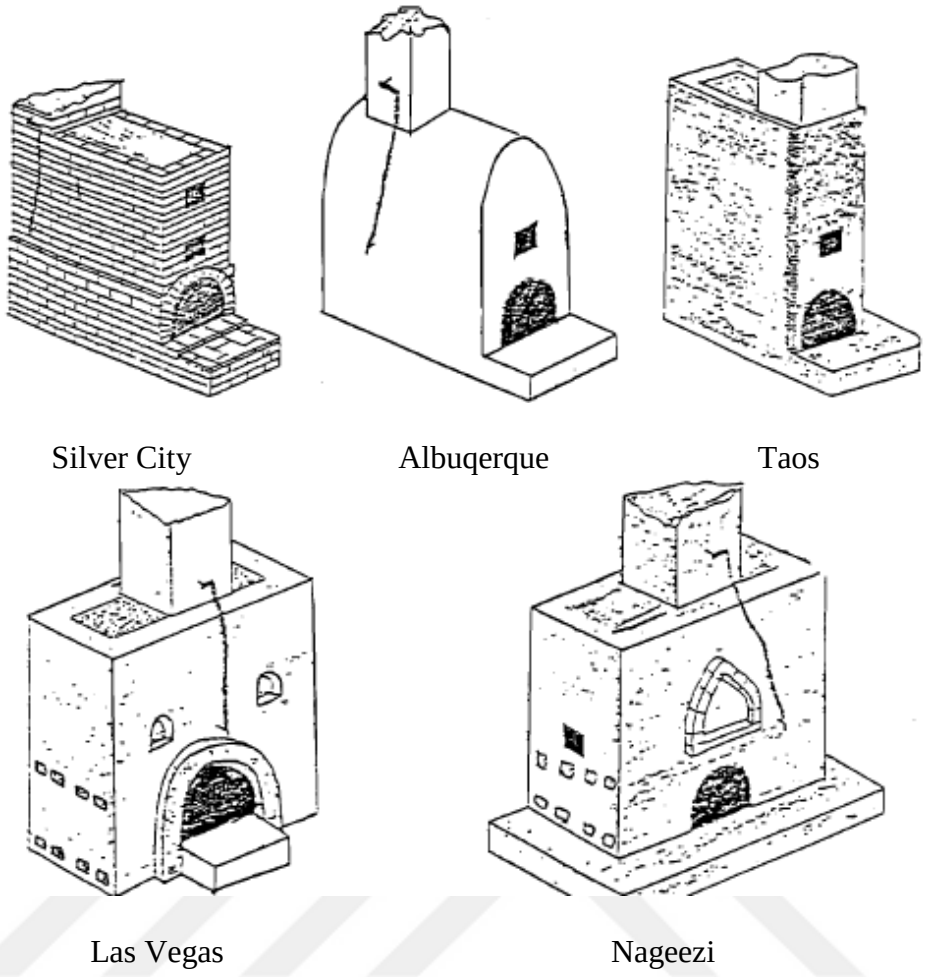

Figure 1.7 : Several types of designed masonry stove by Jay S. Jarpe in New Mexico (Missouri Department of Natural Resources).

The stove design is quite complicated and directly affect the energy performance. The main design elements can be listed as:

- Main body
- Chimney
- Body opening
- Material

The size of the wood stoves varies from small area homes to larger ones. In relation to this condition, heat output capacity of the stoves ranges, significantly. Addition to the size of the wood stove, the smoke circulation path of the heated air is very important to take the advantage of the stoves.

Even the outer design gives an idea about the heat productivity of the stove, it may not be properly done in the most application. Furthermore, the inner design and the utilized material should be considered as key factors of the heat transfer from the stove to the living area.

If the heat distribution can be spread through the whole house, wood stove heating system corresponds the most of the heating demand in the residential buildings. In the low energy needed residential buildings, as passive house, wood stove heating system is adequate to cover heating demand (Feist et al., 2005). In other cases, the occupants should keep the doors opened and accept lower operative temperature. Also, more than one stove can be installed in residential to meet required heating demand (Georges et al., 2014).

1.2.5 Energy efficiency of the wood burning heating stoves

Wood burning stove has several kind of external designs that has significant impact on the energy efficiency of the heat releasing processes.

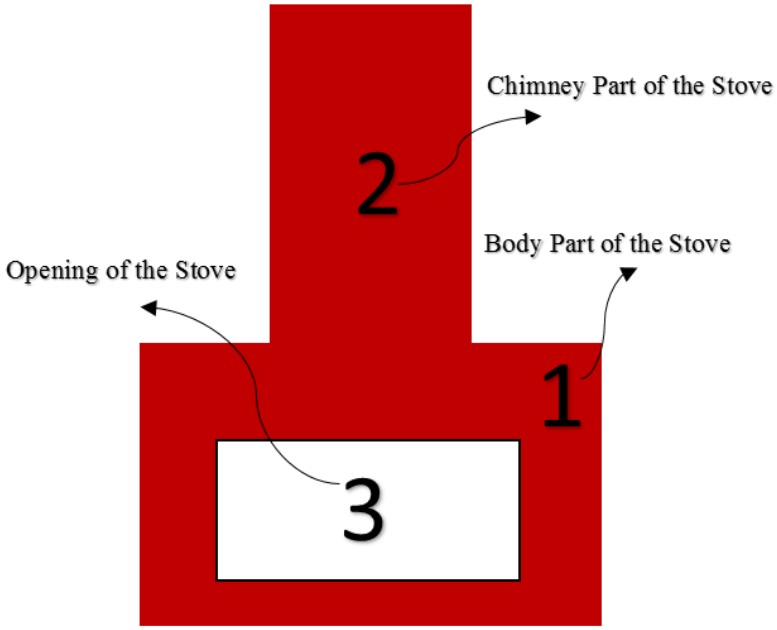

Figure 1.8 : Basic drawing of a stove.

The main factors on the efficiency are:

- Size of the main body
- Size of the chimney
- Design of the of the chimney

- Material
- Body opening size
- Location of the stove in the space
- Hearth opening size
- Fuel type

The efficiency factor is defined to serve the effect of opening of the stove. Stoves are categorized from large opening to controlled damper opening according to the type of burning opening (Grondzik et al., 2010). This categorization refers to the efficiency sorting from poor efficiency to best efficiency. The generated heat load is calculated by considering that efficiency factor. The formula of generated heat load is presented by:

$$\mathrm{kW} = \frac{\mathrm{V} * \mathrm{E} * \mathrm{D} * \mathrm{C}}{\mathrm{T}} \tag{1.1}$$

Where:

V: usable volume of the stove (m^3)

E: Efficiency factor

D: density of the wood ($^{kg}/_{m^3}$)

C: calorific value per kg ($^{kcal}/_{kg}$)

T: Time (hour)

Burning time of the woods is about 8 hours. The burning duration is a determinant factor as the burning period changes the obtained heat output from the stove. Addition to these factors, the generated heat is related to the calorific value of the wood which is needed to be considered in the calculations.

The calorific value depends on moisture content and the wood type of the wood. The important point is to have maximum moisture content as 20% to achieve efficient burning.

The main aim is to keep the heated smoke at the inside of the stove to obtain efficient heat release. Large front opening is classified as poor efficient stove as the heated

smoke flees away from the hearth opening, directly. This situation doesn't let warming up the stove body. If the air entrance is controlled by a damper, it will let the warming up the stove while creating a chance to manage the exit of heated air exit. This is the efficient hearth opening style in the stoves. The efficiency factor is set to 0.5 for this model while it is 0.1 for large front opening model. This shows that the heat output can be enhanced five times more by just changing the hearth opening.

In the figure 1.9, a large front opening is presented. This architecture creates the efficiency factor as 0.1 which is classified as poor.

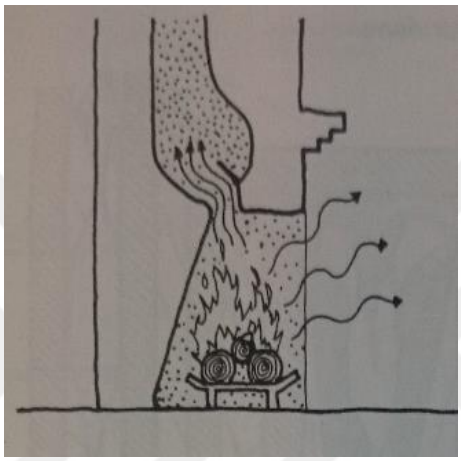

Figure 1.9 : Stove large front opening (Grondzik et al., 2010).

In the figure 1.10, a non-airtight stove opening is shown. Even this model is better than the large front opening design, there is still air leakage around the part and the efficiency factor is classified as 0.2 which is lower.

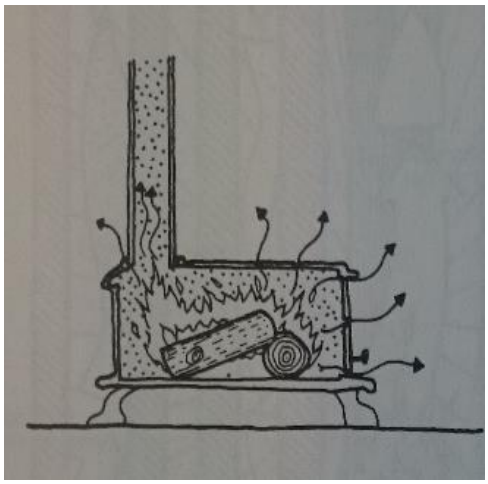

Figure 1.10 : Non-airtight stove Door over opening (Grondzik et al., 2010).

In figure 1.11, almost airtight stove is mentioned. In this model, the air just leaks around the door and the efficiency factor is 0.35 which is considered as better category.

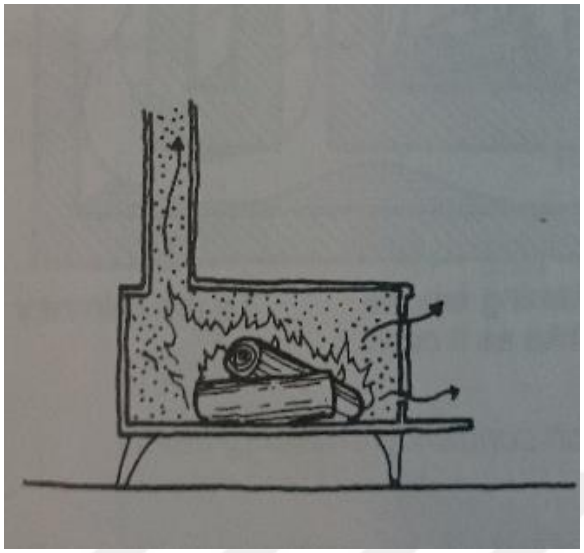

Figure 1.11 : Almost airtight stove (Grondzik et al., 2010).

In figure 1.12, it is seen that a controlled damper is used and the door is gaskated. Based on this model, the efficiency factor is 0.5 which is the best for the all given models.

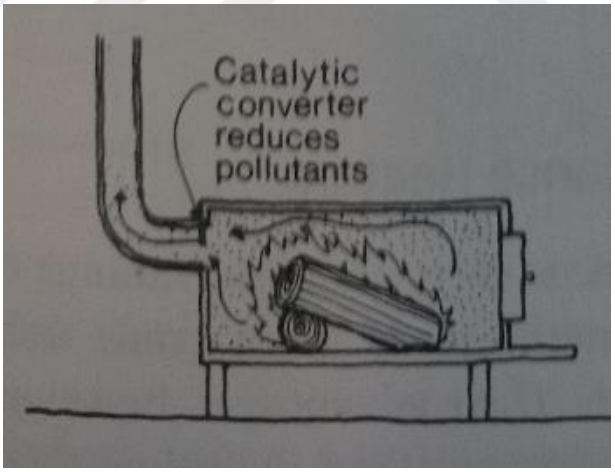

Figure 1.12 : Airtight stove (Grondzik et al., 2010).

As the hearth opening style is important to increase heat output from the stove, the location of the stove is highly considerable as well. The generated heat diffuses through the entire house, however it stays under effect of the heat transfer between internal wall and window.

1.2.6 Placement of the stoves

The heat transfer from building elements has major effect on the heating demand of the houses. The heated air touches these building elements and the released temperature reduces among the house. It should be noted that stove should be enclosed by the building not the external wall to increase the efficiency and the performance (Grondzik et al., 2010). Therefore, the effect of location of the stoves should be considered in the house.

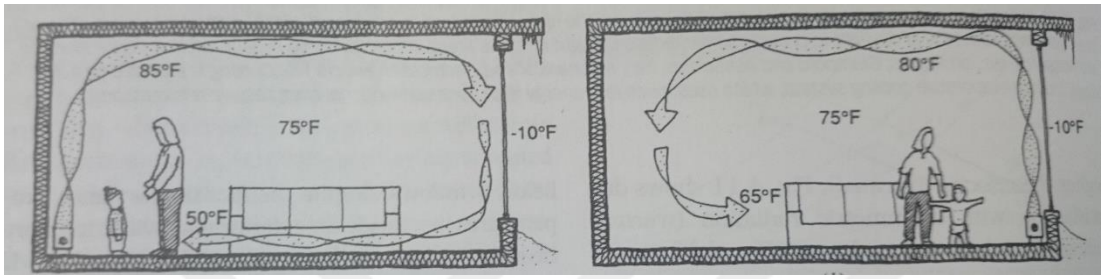

Figure 1.13 : The heat temperature difference in the case of near-by internal wall placement (left) and near-by window placement (right) (Grondzik et al., 2010).

Two different cases are presented in the figure 1.13. The stove is placed near to the inner wall on the right scheme and it is situated near to the window on the left scheme. As the heated air rises up, it contacts to the colder building elements. This causes temperature drop through the house. However, when it is located near to the window, the reducement is less than the other case. The basic reason of this situation is weak insulation.

The low temperature problem of the building elements can be minimized by insulation. Insulation blocks the heat transfer so that the temperature of the walls and windows stay at higher value in the winter sessions. As the insulated building elements are used, the heating demand of the buildings reduces, dramatically. Regarding to the existence of various factors for heat generation and distribution through the house, the fluid flow analysis is needed for the examination of all these effects.

1.2.7 Different chimney models of the stoves

Stoves have several kinds of architectural designs on the exterior surfaces as represented in the previous sections, regarding that, their internal designs show significant details. These different models have major effect on the heat distribution

through to the inside of the house. The heat transfer starts from the combustion part of the stoves. The warmed air rises toward to the chimney outlet.

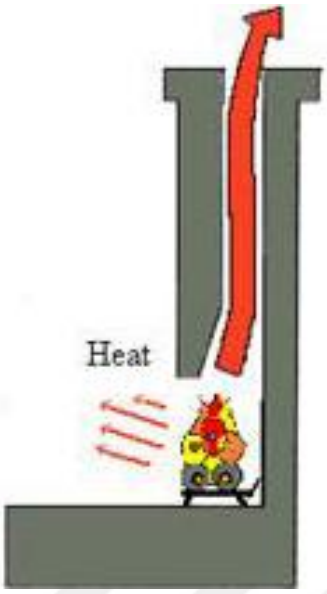

Figure 1.14 : Air movement in the stoves (Url-2).

As the combustion warms the air, warmed air transfers the heat to the outside walls of the stove. After a time, the heated walls warm the inside air in the house. The heat transfer process from stove to the inside air occurs in two ways as convection and radiation (Georges et al., 2014). The heat transfer amount by convection and radiation is related to the material specification as being related to the interior design of stoves.

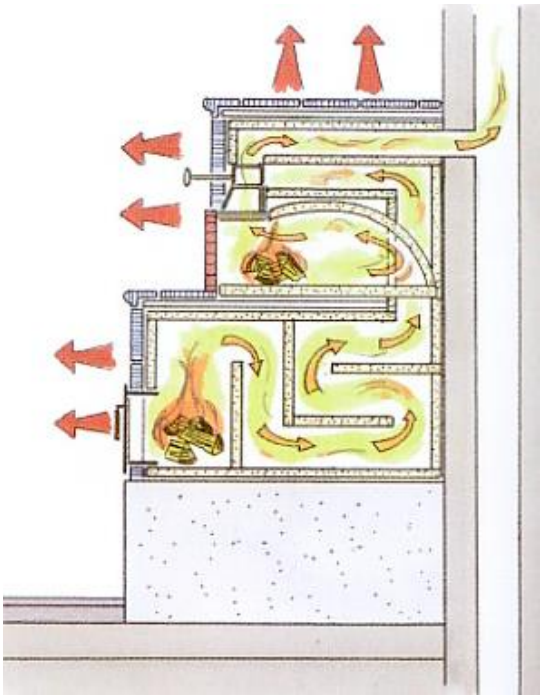

Figure 1.15 : Interior model of the Russian stoves (Url-3).

Russian stove is a type of masonry stove that used in Nordic countries mostly, as mentioned above. In this study, Russian stove was analyzed in the name of energy efficiency and the effect of interior chimney design was investigated with the related material by CFD analysis.

The chimney model of Russian stove is in the form of a labyrinth that allows the circulation of the heated air for a longer period. During this period, more heat transfer ensues from the heated air in contradiction to other stoves.

This different type of masonry stove takes the advantage of flue baffles made of brick and the hot flue gases in S shaped pattern. This serpentine path forces heated air to slow down and increases the length of the flow way. In this way, every centimeter square of the masonry surface absorbs heat from the heated air and this heat transfer process continues as the masonry stoves comes to maximum available temperature. The hot interior surfaces of the masonry wall release their heat through the inside of the building by radiant heating transfer.

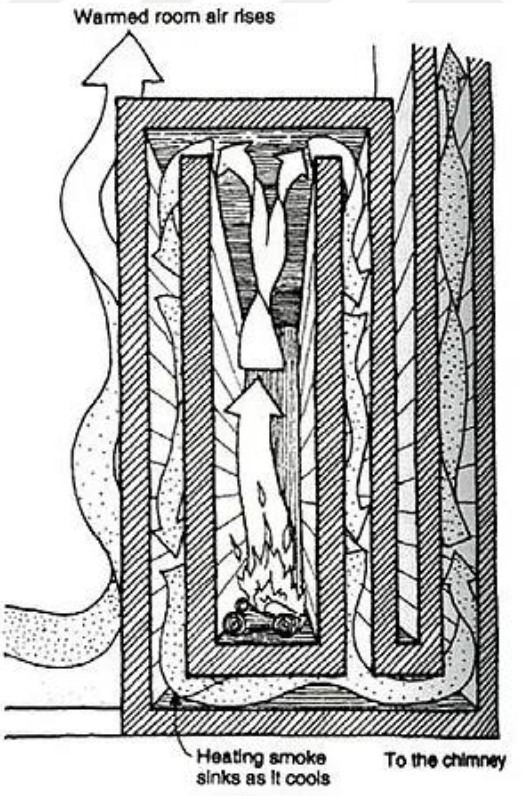

Figure 1.16 : Contraflow system in masonry stove (Hanley et al. ,2005).

The explained heat transfer processes slowly and steady. This provides a very comfortable environment more than an auto-forced hot air furnaces. Furthermore, life

cycle cost of the Russian masonry stove is more advantageous as it uses its fuel so efficiently but the construction cost is mostly same to the other type of masonry stoves.

Russian masonry stove is more environment friendly and produces less pollution than other type of masonry stoves, as it sends less fly ash and unburned gas through to the atmosphere based on its S shape (or labyrinth).

Addition to the unique feature of this internal design, the other usefulness of the Russian stove is needed to be discussed. It should be noted that the design creates a small thermal storage area at the inside of the masonry stove that can be beneficial for passive solar systems. Moreover, it can be adapted for the usage of domestic hot water. The utilization can be supplied from the slowly flowing hot air at the inside of the masonry stove. Furthermore, a part of the stove can be used as oven. Also, the installation of the Russian masonry stove is favorable as it can be placed closer to the walls.

As mentioned above, this stove style releases the heat slowly and it creates more comfortable area than the baseboards. This situation creates better thermal comfort area for the occupant.

The placement of the Russian masonry stove is significantly important, addition to the other mentioned parameters, above. It should be located within the building envelope as the heating is provided by radiant effect. More open space around the stove helps to transfer the radiant heating in the building.

1.2.8 Investigations of the stove's energy performance

In the literature, there are very limited academic research about Russian masonry stove, unfortunately. It is seen that the architectural design is exemplified and the construction processes are shown including each steps by the craftsmen. Also, the energy efficiency and the thermal comfort performance are presented by the users' experiences and remarks.

One of these rare searches was carried out by Department of Architecture – University of Oregon. They evaluated the energy efficiency of contraflow masonry stove by comparing the net heat loss of the home with the consumed energy by stove (Hanley et al., 2005). They analyzed the relation of outside temperature and average inside

temperature for 8 days while operating the contraflow masonry stove. This analysis was performed in a family house located in Pleasant Hill Oregon.

Figure 1.17: Photograph of Barkman family contraflow masonry heater, Pleasant Hill, Oregon (Hanley et al., 2005).

There is an open floor plan in the house that lets the air circulation and spreading through the house. Data loggers were used in the study to obtain the inside air temperature data, in the study. Furthermore, the outside air temperature data were taken to calculate the heat loss and provide the comparison.

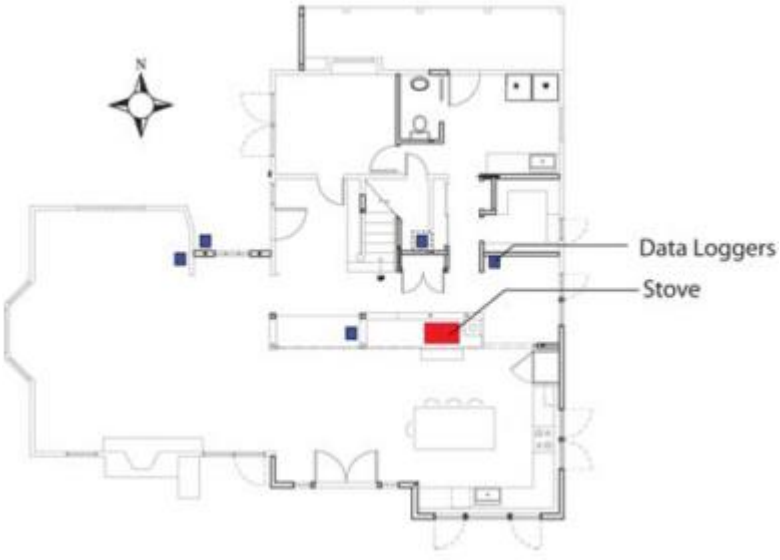

Figure 1.18 : First floor plan of the barkman residence showing the location of the contraflow masonry stove and data loggers (Hanley et al., 2005).

The results show that the indoor air temperature was kept at 18.8°C averagely while the outside temperature fluctuated from 0°C to 11°C. The stove was lit once in a day,

however some days, the home owners didn't need to set fire regarding to the outside temperature. In the figure below, the firing time is shown.

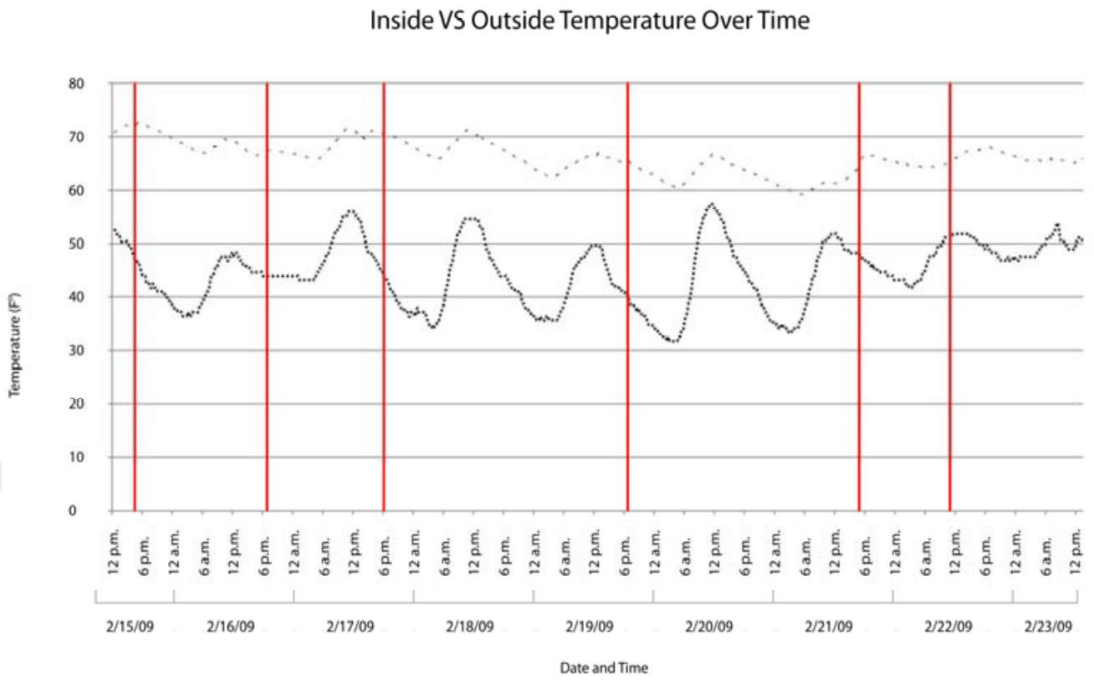

Figure 1.19 : Inside vs outside temperature over time graph with fire burning events (Hanley et al., 2005).

Nearly, 110 kg wood were used in the stove and 2.6 kW heat load was obtained. As mentioned in the study, the net heat loss of the building was calculated as 2.04 kW. Thus, the stove efficiency is reported as 79.5%.

As seen in the study, the masonry contraflow stove (such as Russian, Finnish) works sufficiently to provide the heat demand of the house and keeps the indoor air temperature at the required level as defined by ASHRAE 55.

Another search, which is performed by Georges et al. 2014, investigates the usage of the stoves in a two story passive house. As the heating demand of passive houses is lower than the general building types, the stove usage may cause overheating. The main aim of the study was to evaluate the thermal comfort level on the usage of stove to meet the space heating demand of the passive house building (Georges et al., 2014). Several kind of stoves were examined based on their power levels as 6 kW, 8 kW and 12kW. The study says that if 6 kW or 8 kW stove is preferred, the stove should has power modulation to avoid overheating. However, if 12 kW stove is used, the overheating cannot be prevented even it has power modulation. Addition to this, the results show that the interior door usage is needed to be considered. The opened

interior doors provide better air circulation of heated air and there is no need for power modulation in this condition. Also, the search indicates that one unit of stove is sufficient when the interior doors are kept opened and the occupants are agree about a bit lower operative temperature that stoves cover the heating demand, mostly.

In other search, these researchers examined thermal comfort based on different construction envelope materials. The construction materials were chosen as masonry heavy, wooden heavy and wooden light that these materials differs regarding to their thermal inertia values as 79 MJ/K, 37 MJ/K and 19 MJ/K, relatively (Georges et al., 2013). The case building is a two story residential house and the wood-burning stove is placed on the ground floor. The analysis was performed by assuming the outside weather at -10°C and the simulation was processed for more than 100 hours. At the first period of the analysis the doors were kept closed to see the free floating of the indoor air then the doors were opened to see how flow spreads to other zones on heating period. The results show that the indoor temperature rose so quickly in the coldest room and after then it continued to rise. The indoor air temperature reached to the same value 16°C for all the selected materials. However, in the case of very heavy material, the time duration changed and the heat released slowly by not influencing with much and sudden overheating impact.

Feist W et al., 2005 studied the thermal comfort in a wood stove placed room as a supplementary equipment to ventilation system. The case building is a two story residential building in Stans, Switzerland (Feist et al., 2005). The floors are connected by an open staircase, internally. As mentioned in the study, the set point was arranged to 21°C and the supply air was heated as long as that temperature was not caught. The stove was located in the living room that it was operated for 12 hours. After 12 hours, the heat emittance was assumed to reduce zero. Addition to this internal side configuration, the outside temperature was assumed -2°C. The results show that the room temperature would reach to 27°C, if the stove was fired up once in a day when the interior doors were opened. However, when the interior doors were kept closed, the temperature difference between the rooms was found as 0.5-1°C.

The mentioned studies present the results of final inside air temperature and reveals out the efficiency based on the outside air temperature data by real time. However, the heat distribution can be analyzed by CFD software for the heating systems by considering predicted mean vote (PMV) and predicted percentage of dissatisfied

(PPD) value as addition to the temperature data. Furthermore, the formed temperature gradient, the heat flux from the chimney outlet and the masonry surface can be revealed out by the simulation. Using CFD software provides to visualize the temperature distribution and inside air velocity circulation in the whole building. Heat transfer and energy performance were compared for the different cases by the help of CFD software.

2. METHODOLOGY

In this research, the performance evaluation of the Russian stove was examined based on energy performance and CFD analyses. Therefore, the study was performed by developing 3D model of the stove with its unique characteristics within the building that later converted to energy and CFD models.

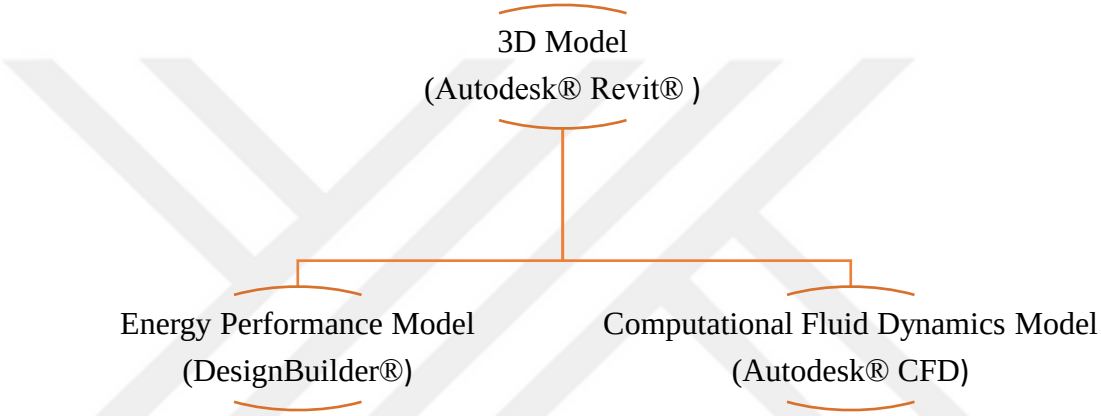

Figure 2.1 : The relation of the models.

The basic step is obtaining the 3D model of the investigated structure. Therefore, Autodesk® Revit® was used to have 3D model and this model was exported to energy performance analysis and CFD analysis to have temperature distribution, heat flux and heating demand of the building.

2.1 Development of the Energy Performance Model

The architectural characteristics of the stove was created within a residential building by utilizing real dimensions. The case structure is a two story building. The thickness of the walls, roof, internal floors and ground floor was identified, furthermore, the windows and the doors were implemented in this section.

In this study, the most important step is to develop 3D model of the Russian stove with its main body and chimney's detailing. As the heat flux and the temperature gradient were investigated mostly, the model was needed to be shaped correctly. The heat

transfer is affected from the outside wall thickness of the stove. This influences the temperature rise of the indoor environment in the heating process of the simulation, directly. If the thickness is defined more than the real designs, it blocks the heat transfer. This situation causes low heat flux and then created heat from the burning process flies up throughout the chimney.

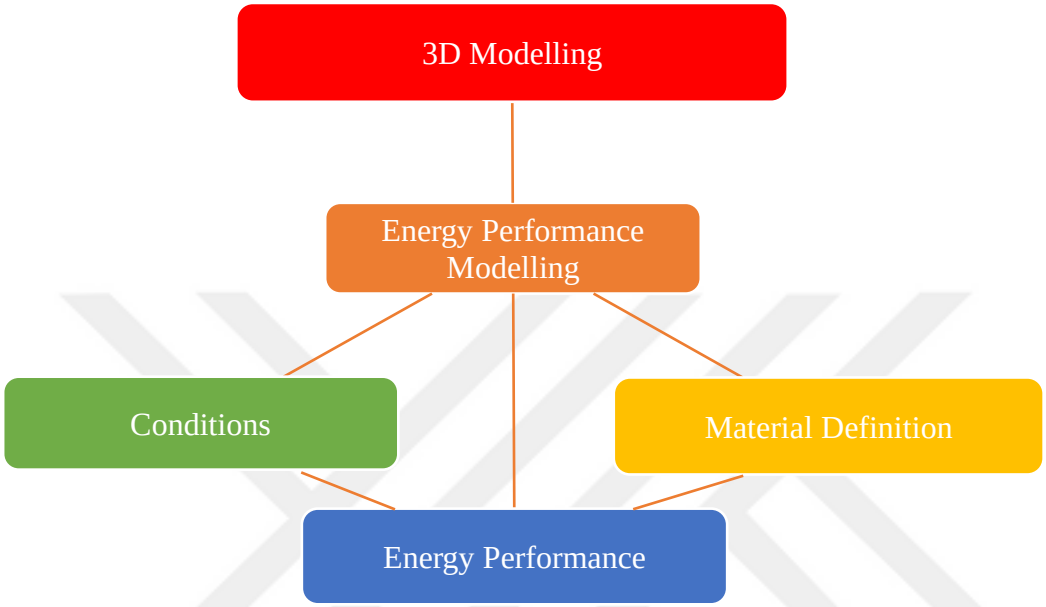

Figure 2.2 : Energy performance analysis concept.

In this purpose, the 3D model of the case building was developed to be used in energy performance simulation software to obtain the heating demand of the building. In this context, the thermal resistance of the case building elements was defined with it specifications such as location, orientation. The overall heating performance of the case building was used to compare the Russian stove heating output which was simulated in a detailed model of CFD within the overall building heating demand.

2.1.1 Preparation of the architectural design

The used 3D modelling software enables the building modelling within the concept of architectural design, structural engineering and "mechanical, electrical and plumbing engineering (MEP)". It creates a building information modelling platform that permits exporting and importing the models from other software.

The developed 3D model of the case building was transferred to CFD programme. In 3D modelling step, a detailed modelling of the Russian stove was done, successfully.

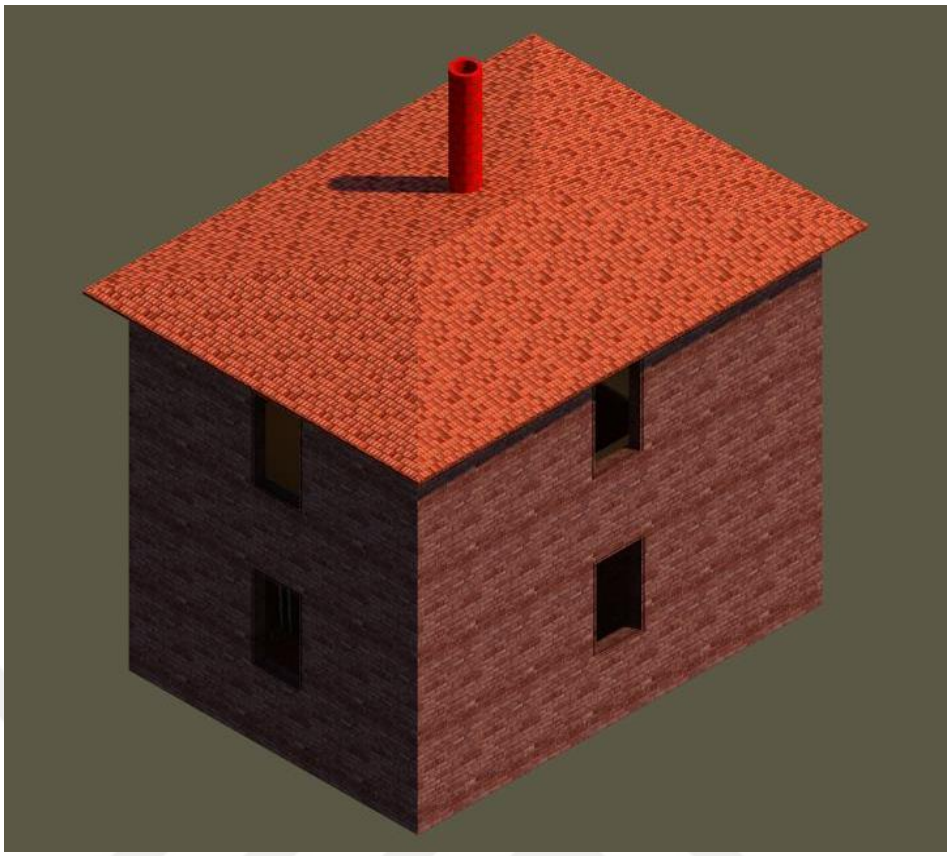

Figure 2.3 : The 3D modelling of the case building.

As, Russian stove has a labyrinth type of chimney, it was needed to be modelled in a specific software. Therefore, the actual dimensions of the building elements were set in 3D model.

This 3D model was exported to the energy performance simulation software to have the heating demand of the building. This result was used in the next step of the study.

2.1.2 Analysis of energy performance

The energy performance of the buildings is calculated by heat transfer formulas including several parameters as presented at the section 3. The material specifications, the heating and cooling systems features, internal climate conditions, outside climate conditions, internal heat gains and solar gains are the basic parameters in these calculations. (Turkish Standardization Institute, 2013) The sunlight angle, shading effects of the neighbor buildings or various outside elements, prevailing wind direction create difficulties to provide these analysis by hand calculations. Besides, the influence of these factors are highly important in the energy performance that can't be neglected.

Energy simulation software is the quickest way to obtain the energy performance calculation. It includes all the mentioned factors in the calculations. Any architectural model with any type of building element can be simulated, quickly and easily in this software.

In this study, the analysis is based on EnergyPlus calculation methods that the software provides a dynamic simulation by presenting all the information about the building elements through a year (Url-4). It calculates the heating and cooling loads with ASHRAE-approved heat balance method by using real hourly weather data of the case region.

The results show the heating load and the heating energy demand of the building monthly and yearly. The peak load was calculated to figure out if the heat generation of the Russian stove covers that peak load demand.

2.1.3 Clarification of TS 825 standardization

The rules of building insulation is regulated by Turkish Standards Institute. Turkish Standards Institute is a national organization and it is responsible for setting the insulation regulation based on Turkey's climatic conditions.

This institute examines the insulation requirements variedly as the climatic conditions differs from region to region.

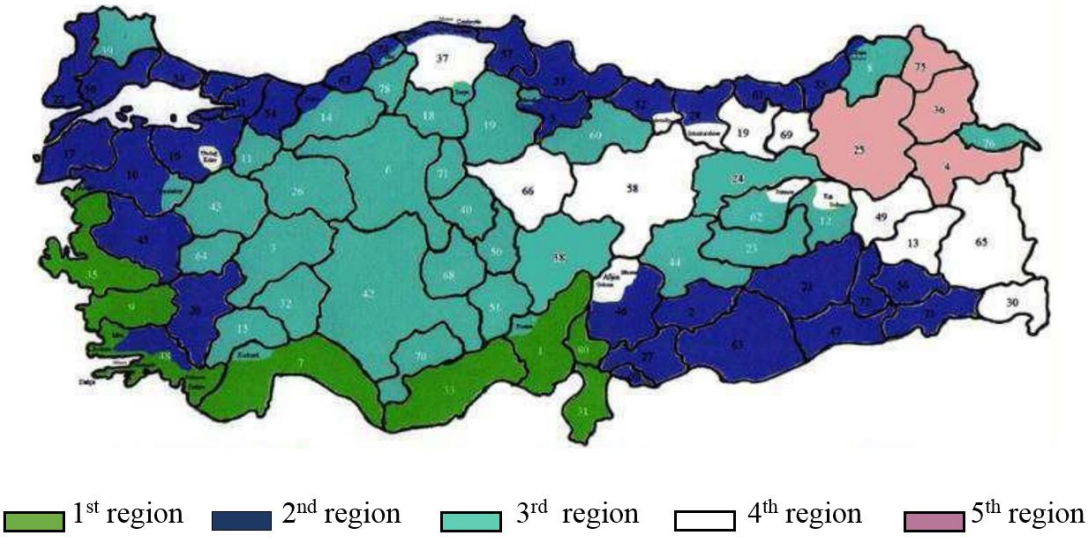

Figure 2.4 : The regional classification of Turkey (Turkish Standardization Institute, 2013).

Thermal insulation requirements for buildings - TS 825 is the guide regulation in this purpose and it includes five climatic regions based on the regional conditions.

Table 2.1 : Thermal insulation requirements based on climatic regions (Turkish Standardization Institute, 2013).

	External Wall ($W/m^2.K$)	Roof ($W/m^2.K$)	Ground Floor ($W/m^2.K$)	Window ($W/m^2.K$)
1. Region	0.66	0.43	0.66	1.8
2. Region	0.57	0.38	0.57	1.8
3. Region	0.48	0.28	0.43	1.8
4. Region	0.38	0.23	0.28	1.8
5. Region	0.36	0.21	0.26	1.8

This study investigated the performance of the Russian stove in a building which is located at Kars. Hence, the thermal insulation requirements were selected based on 5^{th} region.

2.2 Development of the Computational Fluid Dynamics for Heat Flux

In CFD models, the finite element analysis (FEA) method is used. Finite element analysis is a numerical method to find solutions of differential equations by using approximate spatial and temporal derivatives. This derivate is formed by discrete values at spatial grid points and discrete time levels (Kajishima and Taira, 2017). If the grid size and time step are small, the error of the simulations can be at neglected level. Therefore, the real-like results can be obtained in the CFD analysis.

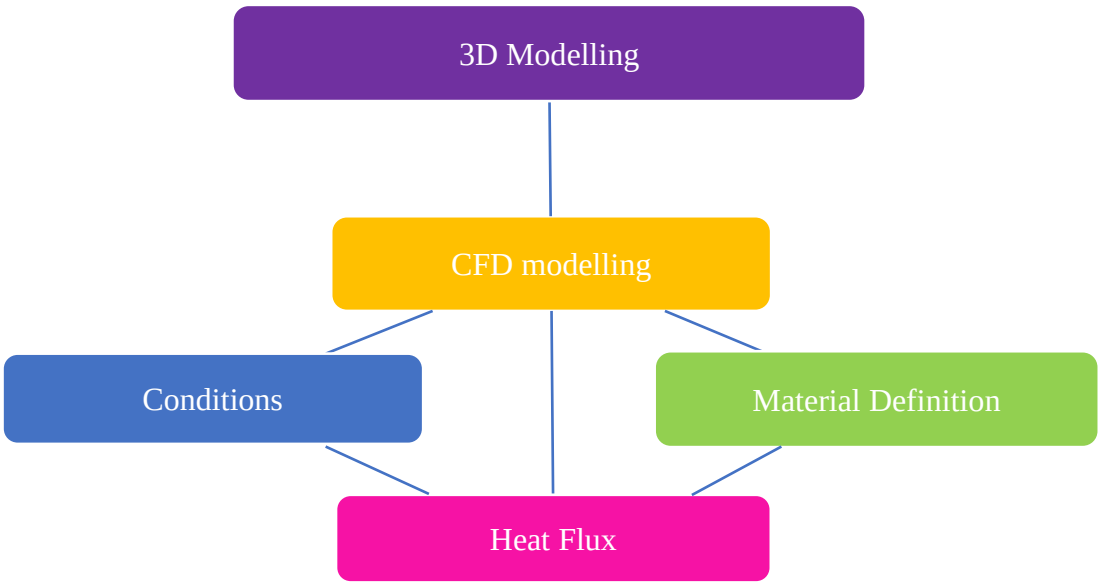

Figure 2.5 : Computational fluid dynamics simulation concept.

The developed 3D model was transferred to CFD model. Since the main service developer of the two model is same, there is an advantage on importing the entire model. In this policy, the missing part formation was avoided. All of the definitions, characterizations and specifications were inserted, successfully. The main data that reveals the results were set in CFD. The material definitions, boundary conditions, initial conditions were given in this section for the model.

2.3 Identification of the Indoor Thermal Comfort Conditions

2.3.1 Application of ASHRAE thermal comfort conditions

In an indoor environment, comfort understanding of occupants is needed to be classified by common principles. Each person has his own comfort scale which influences the indoor environmental design requirements. According to that necessity, thermal comfort principles were investigated by experimentally and the evaluation of the results were converted into standardization. Now, these standards are presented by ASHRAE-55.

In this study, ASHRAE-55 was used to predict the thermal comfort satisfaction. The computational fluid dynamics software has a tool that shows the assessment of the indoor environment.

ASHRAE-55 criticizes the thermal comfort with 6 factors. These factors are:

- Metabolic Rate
- Clothing Insulation
- Air Temperature
- Radiant Temperature
- Air Speed
- Humidity

It should be noted that these factors can change throughout the time, however the point is that these standardization serves the thermal comfort under steady state conditions (American Society of Heating, Refrigerating and Air- Conditioning Engineers, 2010)

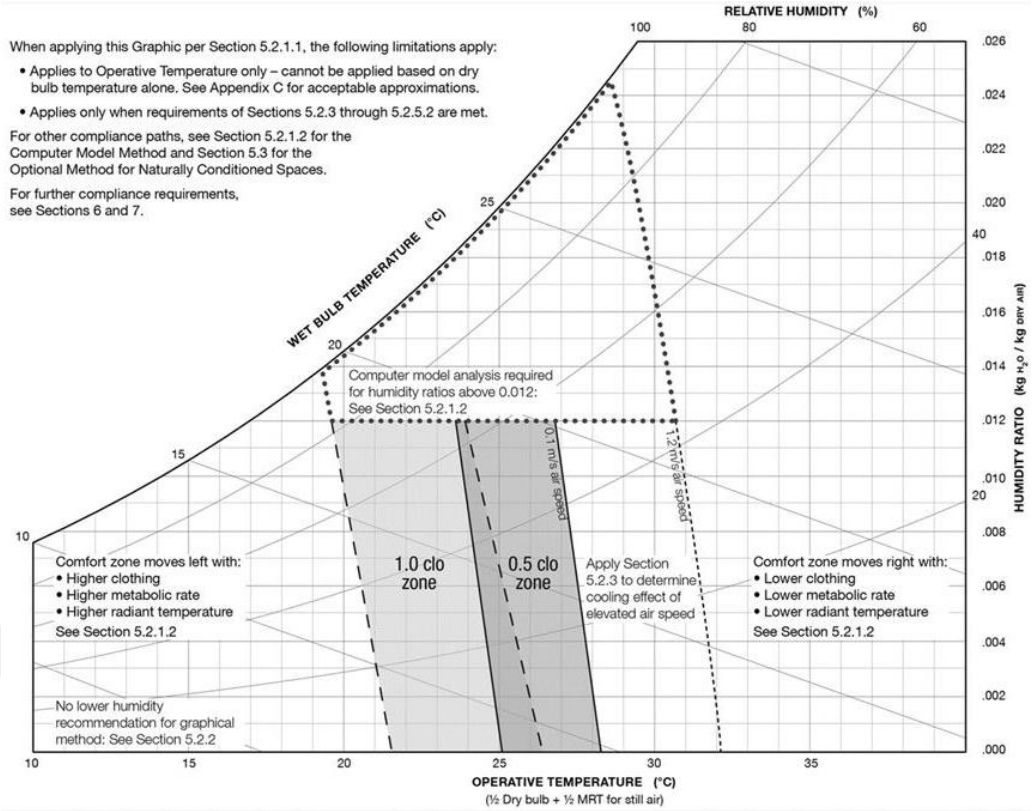

Figure 2.6 : Graphic comfort zone method (American Society of Heating, Refrigerating and Air- Conditioning Engineers, 2010).

Operative temperature varies depending on the humidity, air speed, clothing insulation and metabolic rate. As there are several factors influences the thermal comfort and the operative temperature range, a comfort zone area should be built. The graphic represents the comfort area under conditions of:

- Metabolic rate between 1.0 and 1.3
- Clothing insulation between 0.5 and 1.0.

Operative temperature range is defined in the graphic with 80% of admissibility by the occupants. The rest 20% doesn't feel comfortable because of the dissatisfaction of whole body or a part of the body (American Society of Heating, Refrigerating and Air-Conditioning Engineers, 2010). These situation creates a requirement for a new definition of PMV.

2.3.2 Calculation of Predicted mean vote

Thermal comfort acceptability should address to most of the occupants community. Otherwise, in the context of indoor air quality, thermal comfort standardization cannot

be accepted as succeeded. PMV is an indicator that involves 7 levels. The satisfaction of the occupants is predicted in this principle.

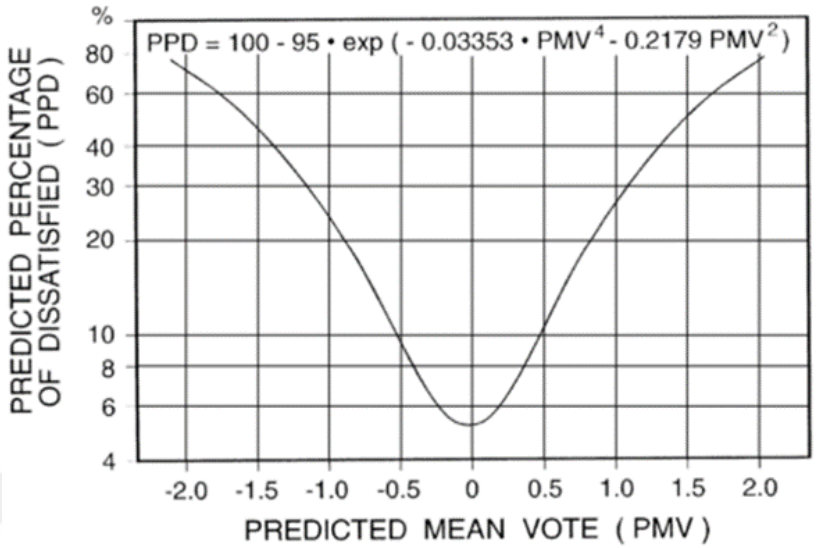

Figure 2.7 : Predicted percentage of dissatisfied as a function of predicted mean vote (American Society of Heating, Refrigerating and Air- Conditioning Engineers, 2010).

PPD is another indicator that shows a quantitative prediction of dissatisfied people for thermal comfort and it is presented in percentage (American Society of Heating, Refrigerating and Air- Conditioning Engineers, 2010). PPD has a direct relation with PMV and they interact each other, directly.

PMV thermal sensation scale can be used in the spaces where the clothing insulation is under 1.5 clo and the metabolic rate is in the range of 1.0 and 2.0 (American Society of Heating, Refrigerating and Air- Conditioning Engineers, 2010). This scale can be presented as:

- +3 hot
- +2 warm
- +1 slightly hot
- 0 neutral
- -1 slightly cool
- -2 cool
- -3 cold

These seven levels indicate that how the indoor environment affects the occupant. If the occupant feels so hot, it is classified by +3 and if he feels so cold, it is classified by -3. As the scale approaches to +3 and -3, PPD increases. It is like symmetrical bell-shaped curve and the dissatisfaction fluctuating as much as in the both conditions.

Table 2.2 : Acceptable thermal environment for general comfort.

PPD	PMV Range
<10	-0.5<PMV<+0.5

PPD is below 10% while the PMV is kept between -0.5 and +0.5. This means that the occupants feel comfortable mostly in this range. Accordingly, figure 2.5, Graphic Comfort Zone Method, indicates the conditions, such as operative temperature, relative humidity, which makes the occupants in the interval of -0.5 and +0.5.

In this study, the thermal comfort was tried to be kept in the desired value regarding to PMV and PPD scope. The Russian stove and the steel casting stove were examined in the frame of mentioned thermal comfort conditions.

3. CASE STUDY: RUSSIAN STOVE

The study has two main analysis to evaluate the stove performance that explained on methodology section as energy performance analysis and CFD analysis.

3.1 Determination of the Energy Performance Analysis

Study goes into examination of heat flux generation and thermal gradient formation depending on time. These factors were investigated in two steps. The first step was performed while the indoor environment temperature was at low temperature and named as heating period. The indoor environment was started to be heated from a specified indoor environment temperature. This process was simulated for Russian stove and steel casting stove, separately.

The second step manages the standby period of the heated environment. As mentioned above, the indoor environment was heated from a low temperature. After getting the desired temperature level, heat source was turned off and standby period was analyzed.

In these two steps, the formation of temperature gradient was observed. Since the examined structure is a two story house, the temperature deployment was aimed to be at the appropriate level in every point of the house. Addition to this, heat flux observation was done according to the materials and the 3D model of the heat source as Russian Stove and steel casting stove.

In the first step, while heating the indoor environment, generated heat flux was observed and the heat flux on the cooling of the indoor environment (while the heat source is turned off) was investigated in real time analysis.

Since these factors are compelling and hard to calculate analytically for the entire house structure, the simulation was run. The model was analyzed including temperature, velocity, heat flux and PMV. To understand the suitability of the results, the study takes the advantage of ASHRAE standards in the discussion of PMV.

3.2 Analysis of Computational Fluid Dynamics

Firestone, firebrick or fireclay is a silica-rich natural clay that can resist to high firing temperature. It doesn't melt, crack, deform, disintegrate and soften.(Cardarelli, 2008) This specification highlights this material's usage on the Russian stove constructions. The temperature of the hearth opening sometimes reaches to 900˚C and the chemical properties of the construction materials becomes highly important in this condition.

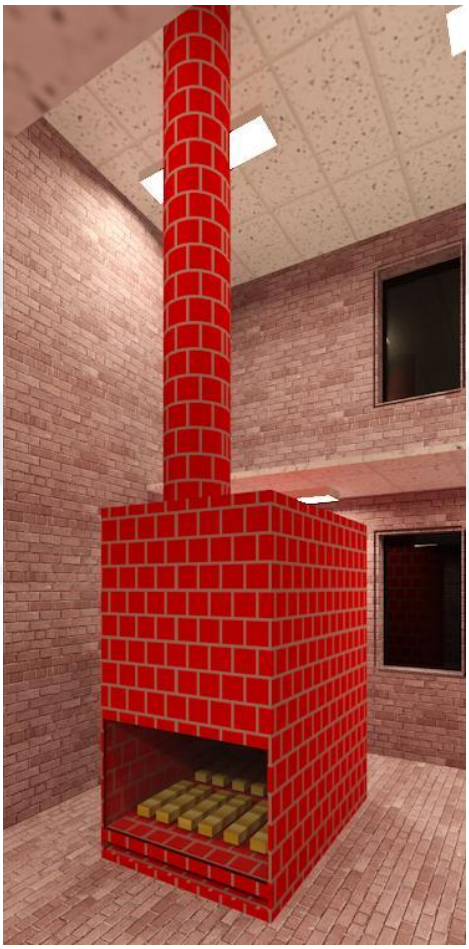

Figure 3.1 : Render imagine of stove.

Firestone has higher specific heat value compared to steel casting. The advantageous of these specification is aimed to be presented by CFD simulation in this study.

CFD software runs the analysis based on the arranged settings. These settings determine the case conditions, requirements and the result outputs. As seen figure below, the settings were defined step by step.

Figure 3.2 : Steps of the computational fluid dynamics analysis.

In this study, two different cases were examined:

- Russian stove
- Steel casting stove

Therefore, the material definition of stoves was done concordantly in the study. However, the material selection of the building elements were kept same to preserve the identical environment conditions as the efficiency of the stove is targeted to be figured out.

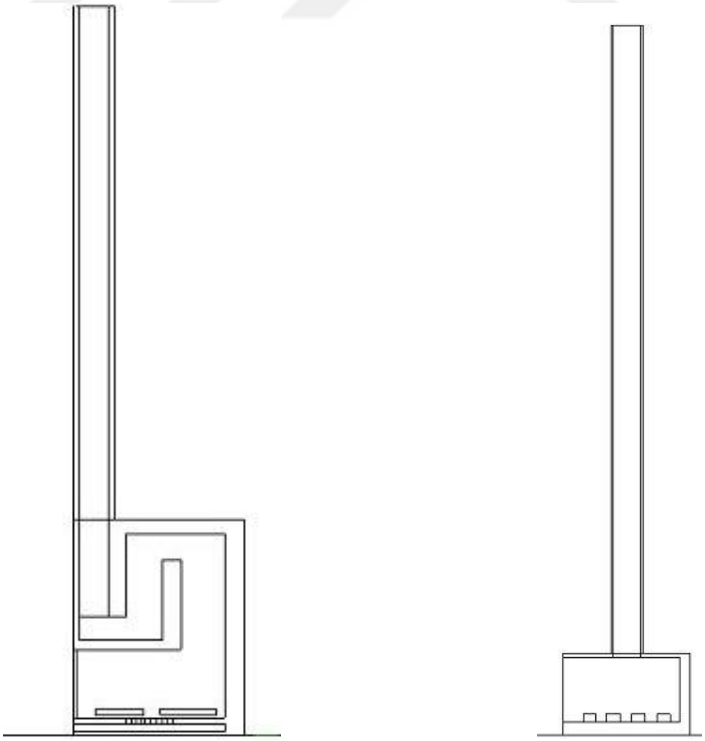

Figure 3.3 : Section view of the stoves**.**

The simulations were constituted within the aim of creating real environmental conditions. As a result of this aim, the most similar results are intended to be obtained according to the real environmental cases.

3.2.1 Assigning the materials

In material designation, the same materials were defined and the identical properties were given in the model by considering the actual conditions and the materials were selected as real building materials.

The used materials can be listed as:

- The roof: Brick
- The external wall: Concreate
- The door and the window frame: Wood
- The Russian stove: Firestone

As this study investigates the heat flux of different kind of stoves, the comparison is executed by different material stove.

The defined material is:

- The compared stove: Steel casting

3.2.2 Assigning the boundary conditions

The thermal comfort satisfaction of the occupants were evaluated by air velocity and temperature of the indoor environmental air in this study. The software uses the heat flow formulas to evaluate these parameters. The inputs of these formulas are identified by boundary conditions.

Boundary conditions are the fundamental of the analysis. It provides the limitations of the calculations and manages the analysis in the related frame of targeted results. The boundary conditions are classified as:

- Steady-state boundary conditions
- Transient boundary conditions

Transient boundary condition is convenient when the analysis is performed for a limited time duration. If duration continues, the results change, accordingly. This kind

of simulations give the outputs regarding to defined parameters through time period. So, the results are observable within defined time step.

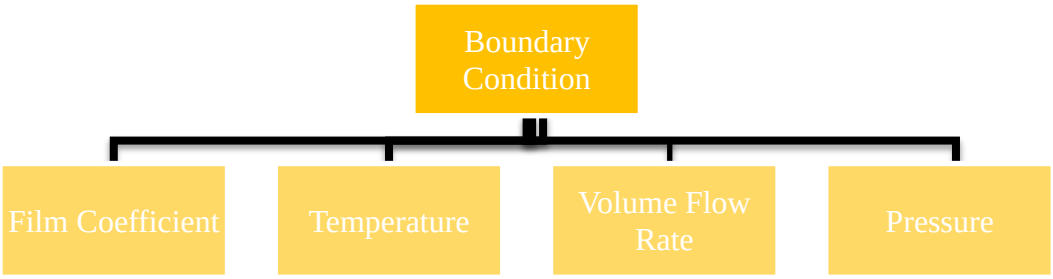

Figure 3.4 : The boundary conditions of the case study.

This research simulates the actual results depending on real time analysis. In this consequences, the boundary conditions were defined as transient boundary conditions.

3.2.2.1 Assigning the film coefficients

Heat transfer is related to temperature difference and the heat transfer coefficient of the building elements. The temperature difference changes based on the outside reference temperature and the initial indoor environmental temperature. As the difference between these two parameters increases, more heat transfer is observed.

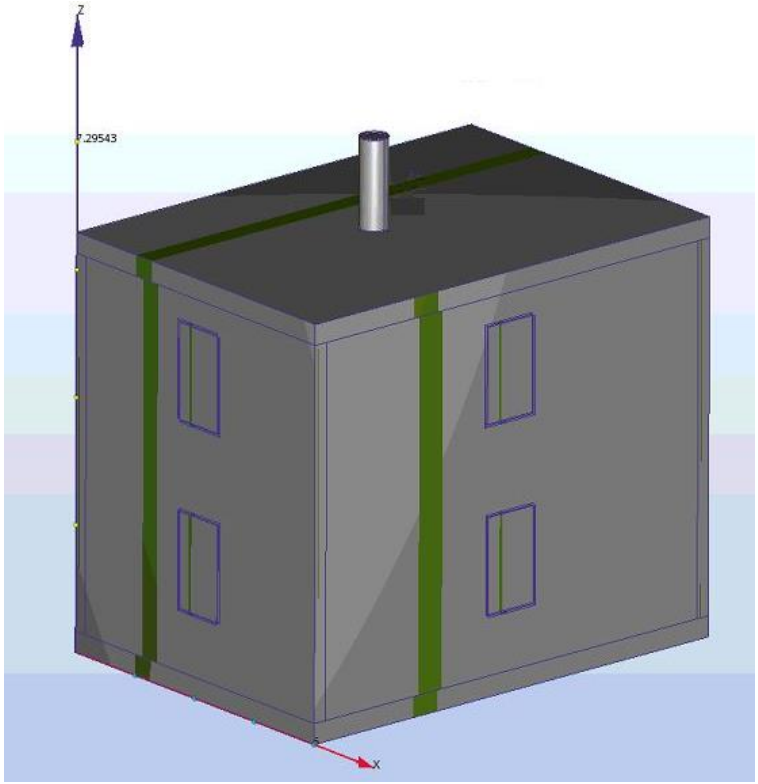

Figure 3.5 : Film coefficient definition on the external wall surfaces.

The heat transfer coefficient of the materials is called as u-value. The u-value of the building elements matters to decrease and to avoid the heat transfer, extremely. In this study, the u-value was defined for any building element which is in the contact with external air domain.

Table 3.1 : The film coefficient values of the building elements.

Building Element	Film Coefficient Value ($W/m^2.K$)
External Wall	0.36
Roof	0.21
Ground Floor	0.36
Window	1.8

The film coefficients are specified in the line with TS 825 standards. TS 825 standards determines the most available film coefficient value based on the climatic conditions. The building location was assumed in fifth climatic region and suitable values were defined in the simulations, as mentioned in the previous sections.

3.2.2.2 Assigning the temperature values

The heating source is wood in the Russian stove and the indoor air temperature rises accordingly as the wood burns. The heat generation output is examined to analyze the efficiency of the stove. Thus, the heat generation was not defined.

The other way to obtain heat generation process is to determine temperature of the burning wood as actualizes real condition. So, the temperature input was given to the wood logs.

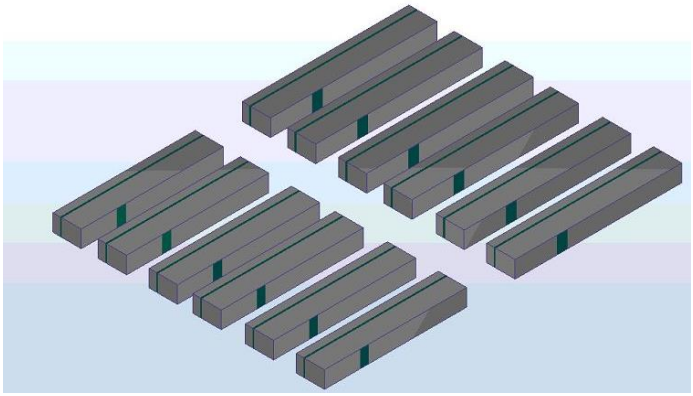

Figure 3.6 : Temperature value definition of wood blocks.

The temperature was defined by linear transient method. This method provides the real temperature rise condition as in real case. As this study investigates the thermal

comfort conditions in the winter session, the initial temperature of the wood was defined as 12˚C. However, as the burning process starts, the wood temperature reaches to 450˚C after 30 minutes (1800 Seconds). So, the real temperature change case was created by these definition method to figure out the exact thermal comfort results.

Table 3.2 : The temperature of the woods.

Time (Seconds)	Temperature (˚C)
0	12
1800	450

3.2.2.3 Assigning the infiltration rate

The air circulation is caused by infiltration effect in the buildings. The external air enters and internal air exists from the buildings. These movements are caused form natural ventilation. This effect must be defined in the simulation models to figure out the energy performance of the buildings. Otherwise, the heat loss (winter session) and heat gain (summer session) becomes ignored in the evaluations.

The natural ventilation was defined by infiltration rate in the model. The window frames were defined as the air entrance region and this condition was determined with volume flow rate.

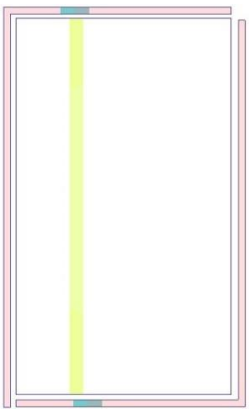

Figure 3.7 : Volume flow rate definition on the window frames.

The energy consumption is effected by infiltration as mentioned above. Addition to the flow rate of the air entrance, the temperature of the entering air must be taken in consideration.

Table 3.3 : Infiltration specifications of the case building.

Volume Flow Rate ($m^3/h.m^2$)	Temperature (˚C)
3	0

The case study was investigated under winter conditions, therefore the outside temperature was set at 0˚C. This condition was defined for the entering air addition to the volume flow rate.

The thermal comfort evaluation is actualized by PMV assessment. So, the human figures were placed in the building to see the thermal comfort results. PMV result shows the indoor temperature satisfaction based on the human temperature. Hence, the human temperature was needed to be defined in the simulation.

Table 3.4 : Human temperature.

Element	Temperature (˚C)
Human	36.5

Definition of the human body temperature is very important. Because, if the body temperature is not specified as boundary condition, the simulation assumes the body temperature as 0˚C. Regarding to this assumption, PMV results may be presented falsely.

3.2.2.4 Assigning the pressure

The heated air rises based on the density change and it tries to find a way to exit through the chimney. Otherwise, the smoke may move backwards all along the house and causes poisoning. Therefore, an exit must be defined in the analysis.

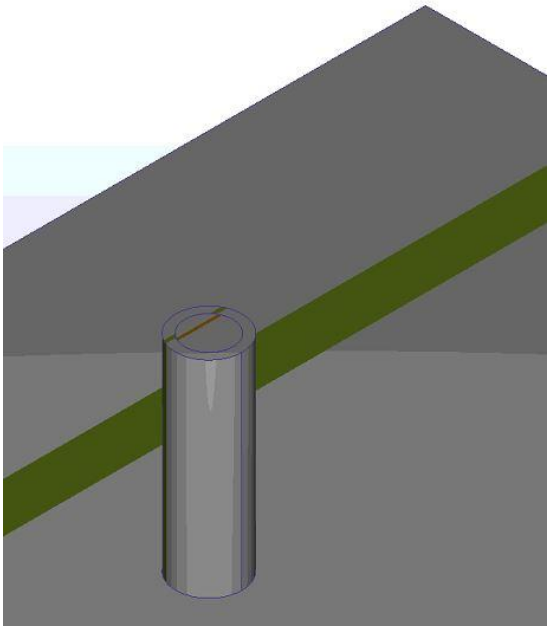

Figure 3.8 : Pressure definition on the outlet of the chimney.

The chimney exit was set by pressure difference in the simulation, so, pressure outlet was given by 0 Pa.

Table 3.5 : The chimney outlet.

Input	Pressure (Pa)
Pressure Outlet	0

3.2.3 Assigning the initial conditions

The final results are calculated considering the initial value of the indoor air temperature and the building elements. Initial temperature value of the each building element was defined in the simulation.

Table 3.6 : Initial conditions of the fluid dynamics analysis.

Building Element	Initial Temperature (˚C)
External Wall	7
Roof	7
Window	7
Ground Floor	7
Ceiling	7
Indoor Air	12

Initial temperature value of the each building element was defined in the simulation.

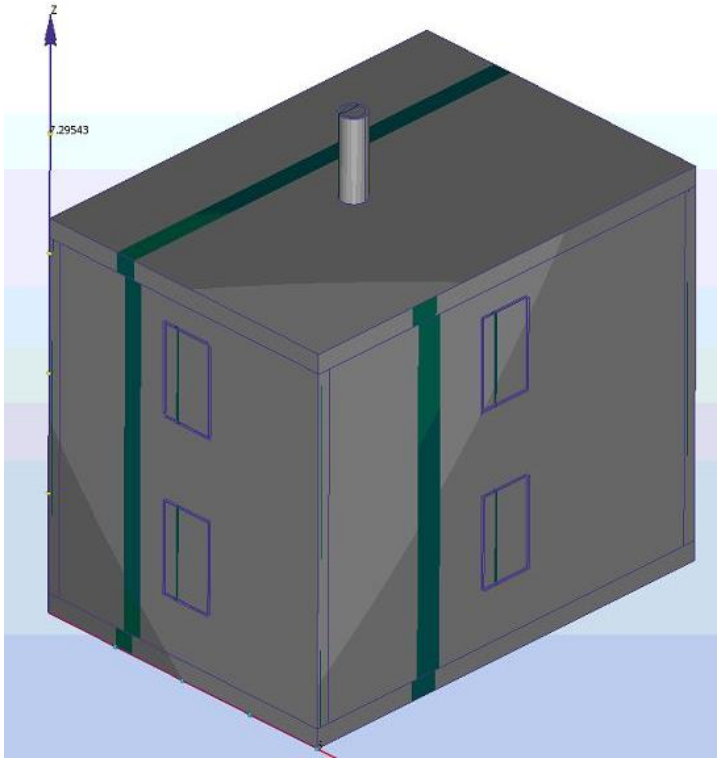

Figure 3.9 : Initial condition definition on the building.

The final results are highly affected from the initial conditions, so, these inputs are specified appropriately as the real existing conditions.

3.2.4 Description of mesh

In the simulations, the models are presented in 2D or 3D geometry. However, the software consider the model in small pieces rather than a whole part.

In this purpose, firstly the entire body is broken into small pieces that these are called **elements**. These elements have several number of corners based on their geometry that these corners are called as **nodes**. By the coming together of elements and nodes, the **mesh** model is obtained in the simulation (Url-5).

3.2.4.1 Determination of the element types

In CFD programme, tetrahedral element type is used on the mesh process, generally (Url-5). However, the prism element type is created on the wall layers. Except the wall layers, all the rest is meshed by tetrahedral element type.

Tetrahedral element type

The 4 node tetrahedral element can be used to model 3D geometries. Each node has 5 degrees of freedom for laminar flow: U, V, W, P, T and 7 degrees of freedom for turbulent flows: U, V, W, P, T, k,ε (Url-5).

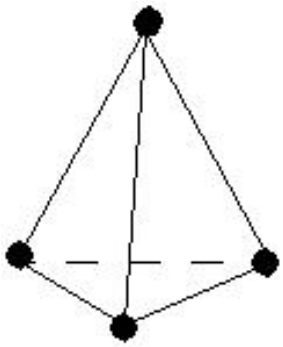

Figure 3.10 : Tetrahedral element and the nodes (Url-5).

Pyramid element type

The 5 node prism element can be used to model 3D geometries. Each node has 5 degrees of freedom for laminar flow: U, V, W, P, T and 7 degrees of freedom for turbulent flows: U, V, W, P, T, k,ε (Url-5).

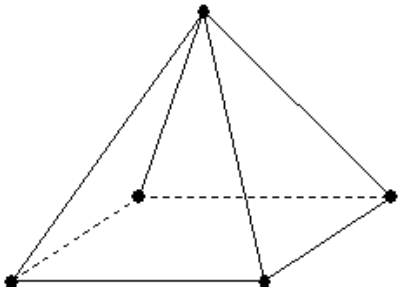

Figure 3.11 : Pyramid element and the nodes (Url-5).

3.2.4.2 Application of mesh enhancement

The mesh sizing is very important to obtain real like results in the simulations that it provides the reliability in the outcomes. Mostly, any CFD software has its own automatic mesh sizing option. However, they just provide an idea about the results. If the real like results are aimed to be achieved, mesh enhancement study is a must.

Mesh enhancement study is acquired by repeating the same model with a better mesh application. Therefore, till getting the result difference as 5%, the mesh enhancement is needed to be repeated.

In this study, the mesh enhancement was performed by refining the mesh in each new model. As one model finished the convergence, it was cloned and the mesh was refined to 0.7. After finishing the convergence, the results were compared. If the difference is more than 5%, the simulation was cloned and the mesh was improved to 0.7, again. This application was proceeded until the difference was reduced to 5% in each measurement point.

The execution of this application provides the dependability and proves the functionality of the results and the simulated model.

3.2.5 Definition of the transient solution parameters

In this study, the simulation was performed by transient solution mode as mentioned in the previous sections. In the application of transient solution mode, additional solution parameters are needed to be defined when compared to steady-state solution mode.

In CFD analysis:

- Time step size (seconds)
- Stop time (seconds)

- Number of inner iterations
- Number of time steps to run are the determinant parameters for transient simulation.

Time step size defines the time interval of the simulation time. The selection of suitable time step size is important to obtain the accuracy on the results. If the time steps size is relatively large, the data lost is observed. Because it would be exceeding the appropriate time scale of the flow.

The time step size is calculated by considering the actual fluid movement time. If the total travel time of the fluid is x seconds in a case, 1/20th of this time should be defined in the simulation as time step size. As an example:

If a fluid passes 2 m distance with 0.1 m/s velocity, the movement time of the fluid is calculated as 20 seconds. However, 1/20th of 20 seconds, which is 1 second, should be defined as time step size.

Stop time specifies the entire simulation time of the case. If 10 minutes of the fluid movement is aimed to be analyzed, the stop time should be defined as 600 seconds in stop time section.

Number of inner iterations identifies the required iteration value per iteration. Based on the convergence plot, the number of inner iterations can be arranged.

Number of time steps examines the total amount of the required time steps for the entire simulation time and it is calculated by using time step size, inner iteration and stop time. It can be expressed as:

$$\text{Number of time steps} = \frac{\text{stop time x inner iterations}}{\text{time step size}} \tag{3.1}$$

All of the mentioned parameters are highly important to obtain realistic results in the simulations. In this study, the heating period was investigated for 10 hours. Hence, the related transient setup parameters can be found in the below table:

Table 3.7 : The parameters of transient analysis.

Parameters	The value
Time Step Size	3
Stop Time	36000
Inner Iteration	1
Number of Time Steps	12000

3.2.6 Selection of the solution method

There are several techniques to form the finite-difference equations and Taylor series expansions or polynomial approximations. They are mostly used in finite element analysis (Kajishima and Taira, 2017). The Taylor series can be expressed as:

$$f_k = f_j + \sum_{m=1}^{\infty} \frac{(x_k - x_j)^m}{m!} (f_j)^{(m)} \tag{3.2}$$

The accuracy of the CFD analysis is related to the discrete time levels as mentioned above. The time step size (time rate change) is highly important to obtain real-like results. Advection-diffusion equation uses Navier-Stokes equations.

3.2.6.1 Categorization of the turbulence model

Turbulence is a fluid flow phenomenon and it is personified by a few factors as:

- Unsteadiness
- Complex and irregular fluid motions
- Wide range of physical scales fluid motions
- Rapid mixing of passive contaminants (Recktenwald, 2009)

More than these definitions, the characteristic behaviors of the turbulent flow are needed to be described to understand the act of the flow. Turbulence model can be classified based on main stress model and subcategorization. Turbulence stress model is defined by major classification as:

1) Reynolds stress model
2) Algebraic stress model
3) Eddy viscosity model

The subcategorization is developed in four headlines as:

Subcategorization 1 specifies the number of partial-differential equations for the identification of the turbulent scales.

Subcategorization 2 defines the number of ordinary-differential or other non-partial differential model equations for the identification of the turbulent scales.

Subcategorization 3 describes the general type of fluid of the model:

1) Incompressible/compressible fluid model
2) Compressible fluid model
3) Incompressible fluid model

Subcategorization 4 characterizes the treatment of the near wall-boundary flow:

1) Integration to the wall
2) Wall function
3) Algebraic with matching point
4) Switch to one-equation near the wall (Bardina et al., 1997)

Reynolds number is a dimensionless unit that defines ratio of the inertia forces to the viscosity forces of the flows (Incropera et al., 2007a). Reynolds number is related to:

$$Re_x = \frac{\rho * u_\infty * x}{\mu} \tag{3.3}$$

Where:

ρ= Density of the flow (kg/m^3)

u_∞= Velocity of the flow (m/s)

x= Characteristic length (m)

μ= Dynamic viscosity ($kg/m.s$)

If the Reynolds number is high, the instantaneous and random change of the flow cannot be blocked by viscous forces. Reversely, if the Reynolds number is low, viscous forces repress the inertia forces and keep the flow in the laminar form.

If Reynolds number lower than 2000, the flow is classified as laminar and if the Reynold number is more than 4000, it is defined as turbulent flow. The transition flow is shaped when the Reynolds number is in the range of 2000 and 4000 (Incropera et al., 2007b).

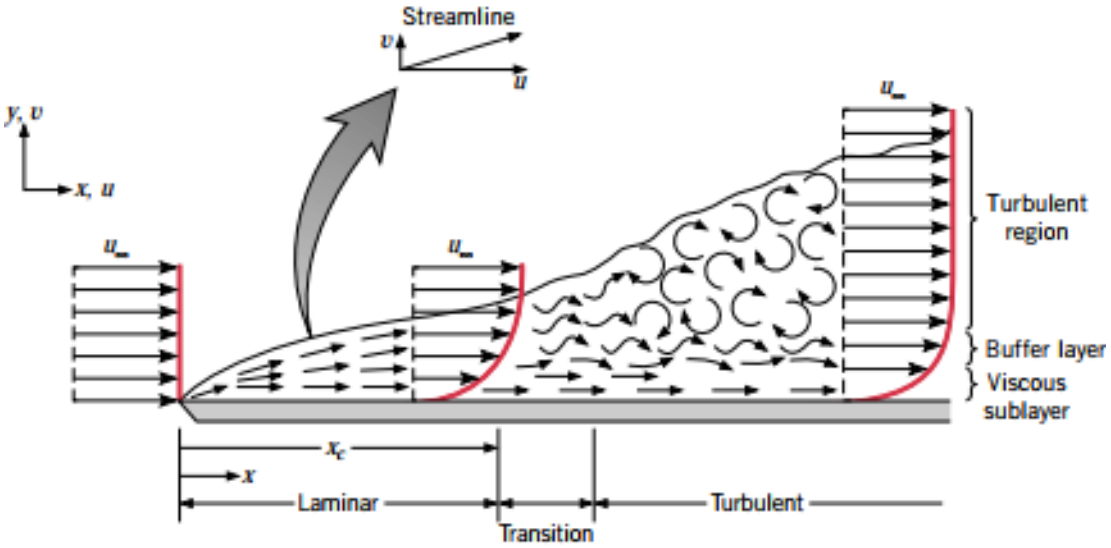

Figure 3.12 : Velocity boundary layer development on a flat plate (Incropera et al., 2007b).

k-ε Turbulence Model

In the CFD simulations, turbulence flow is needed to be defined by a certain turbulence model. K-epsilon is one of this turbulence models.

K-epsilon turbulence model is applicable for the most of the simulation models. It is a kind of default model that it is applicable for many cases. So, the general output results of the cases can be obtained, easily (Url-6). Most of these cases are related to conventional upwind discretization for the advection terms (Schnipke, 1986). In this method, k symbolizes turbulent kinematic energy, while ε (Epsilon) shows dissipation rate (Scott-Pomerantz, 2004).

Low Re k- ε

Low Re k-epsilon model is another turbulence model and it is very helpful to simulate low speed turbulent flows. In the cases of Low Re k-epsilon model, Reynolds number range should be between 1500 and 5000. This model is suitable for natural convection cases (Bouncy driven). Addition to this, if natural convection flow is rarely seen in turbulent flow form, this turbulence model can be used, still. Therefore, it can be used for both slow and high speed regions (Url-5).

However, there some points needed to be cared when Low Re k-epsilon model is preferred:

-As this model doesn't use wall function, wall layers minimum must be set to 5.

-The mesh is needed to be improved carefully rather than other cases.

-Low Re k-epsilon model is less stable when compared to k-epsilon model. Based on this situation, more iterations are needed to obtain convergence.

-It should be noted that, if the model is needed to change from k-epsilon to Low Re k epsilon mode, the simulation time increases, muchly.

Finally, reversely the negative sides of this model, it gives the similar results of laminar flow for slow speed flows, while it gives the same results of k-epsilon flow for high speed flows as an advantage (Url-6).

CFD simulation is run by using the given fluid dynamics formulas. The formulas change based on the simulated case as mentioned above. In this study, there is no auto-forced flow that the case flow is natural convection formed by infiltration. Addition to this, high temperature value in the furnace body causes density difference. This density difference is the other reason of natural convection. Therefore, the turbulence flow was selected as Low Re k-epsilon method based on natural convection criteria.

3.2.6.2 Development of the governing equations

Motion of the fluid has a complex nature based on its three dimensional structure and time dependent frame. The dynamic change of inputs and outputs creates difficulty on the integration of the inconstant variables. The usage of the partial differential equations are included on the definition of the fluid motion.

Fluid motion includes heat transfer, pressure changes and velocity fluctuations. The most appropriate way on the description of these parameters are provided by governing equations. CFD software takes the advantage of these governing equation during the simulations.

The governing equations are based on the continuity equations, Navier-Stokes equations and energy equations and these equations are applicable for both of the laminar and turbulent flow (Bardina et al., 1997) (Url-6).

Continuity equation:

$$\frac{\partial \rho}{\partial t} + \frac{\partial u}{\partial x} + \frac{\partial \rho v}{\partial y} + \frac{\partial \rho w}{\partial z} = 0 \qquad (3.4)$$

X-momentum equation

$$\rho\frac{\partial U}{\partial t}+\rho U\frac{\partial U}{\partial x}+\rho V\frac{\partial U}{\partial y}+\rho W\frac{\partial U}{\partial z} = \rho g_x-\frac{\partial P}{\partial x}+\frac{\partial}{\partial x}\left[2\mu\frac{\partial U}{\partial x}-\rho uu\right] + \frac{\partial}{\partial y}\left[\mu\left(\frac{\partial U}{\partial y}+\frac{\partial V}{\partial x}\right)-\rho uv\right]+\frac{\partial}{\partial z}\left[\mu\left(\frac{\partial U}{\partial z}+\frac{\partial W}{\partial x}\right)-\rho uw\right] \quad (3.5)$$

Y-momentum equation:

$$\rho\frac{\partial V}{\partial t}+\rho U\frac{\partial V}{\partial x}+\rho V\frac{\partial V}{\partial y}+\rho W\frac{\partial V}{\partial z} = p\rho-\frac{\partial P}{\partial y}+\frac{\partial}{\partial x}\left[\mu(\frac{\partial U}{\partial y}+\frac{\partial V}{\partial x}-\rho uv\right] + \frac{\partial}{\partial y}\left[2\mu\frac{\partial V}{\partial y}-\rho vv\right]+\frac{\partial}{\partial z}\left[\mu\left(\frac{\partial V}{\partial z}+\frac{\partial W}{\partial y}\right)-\rho vw\right] \quad (3.6)$$

Z-momentum equation:

$$\rho\frac{\partial W}{\partial t}+\rho U\frac{\partial W}{\partial x}+\rho V\frac{\partial W}{\partial y}+\rho W\frac{\partial W}{\partial z} = \rho g_z-\frac{\partial P}{\partial z}+\frac{\partial}{\partial x}\left[\mu\left(\frac{\partial U}{\partial z}+\frac{\partial W}{\partial x}\right)-\rho uw\right] + \frac{\partial}{\partial y}\left[\mu\left(\frac{\partial V}{\partial z}+\frac{\partial W}{\partial y}\right)-\rho vw\right]+\frac{\partial}{\partial z}\left[2\mu\frac{\partial W}{\partial z}-\rho ww\right] \quad (3.7)$$

Energy Equation:

$$\rho C_p\frac{\partial T}{\partial t}+\rho C_p U\frac{\partial T}{\partial x}+\rho C_p V\frac{\partial T}{\partial y}+\rho C_p W\frac{\partial T}{\partial z} = \frac{\partial}{\partial x}\left[k\frac{\partial T}{\partial x}-\rho C_p uT^{\iota}\right]+\frac{\partial}{\partial y}\left[k\frac{\partial T}{\partial y}-\rho C_p vT^{\iota}\right] + \frac{\partial}{\partial z}\left[k\frac{\partial T}{\partial z}-\rho C_p wT^{\iota}\right]+q_V \quad (3.8)$$

Where:

C_p: Constant pressure specific heat

g_x, g_y, g_z= Gravitational acceleration in x, y, z directions ($^{m}/_{s^2}$)

h: Enthalpy (J)

k: Thermal conductivity ($^{W}/_{mK}$)

p: Pressure (Pa)

q_V: Volumetric heat source ($^{kW}/_{m^3}$)

T: Temperature (C°)

t: Time (Second)

u: Velocity component in x-direction ($^{m}/_{s}$)

v: Velocity component in y-direction ($^{m}/_{s}$)

w: Velocity component in z-direction ($^{m}/_{s}$)

μ: Viscosity ($^{m^2}/_{s}$)

ρ: Density ($^{kg}/_{m^3}$)

As mentioned on the previous sections, k value presents turbulent kinematic energy while ε symbolizes the dissipation rate (Jagadeesh, P. and Murali, K., 2005). In the context of Low Re number turbulence model, the used k- ε equations are given as (Url-7):

$$\frac{\partial}{\partial t}(\rho k) + \frac{\partial}{\partial x_j}[\rho k u_j - (\mu + \frac{\mu_t}{\sigma_k})\frac{\partial k}{\partial x_j} = P - \rho\varepsilon - \rho D \tag{3.9}$$

$$\frac{\partial}{\partial t}(\rho\varepsilon + \frac{\partial}{\partial x_j}[\rho\varepsilon u_j - (\mu + \frac{\mu_t}{\sigma_\varepsilon})\frac{\partial \varepsilon}{\partial x_j} = (C_{\varepsilon 1} f_1 P - C_{\epsilon 2} f_2 \rho\varepsilon)\frac{\epsilon}{k} + \rho E \tag{3.10}$$

Where:

$$\mu_t = C_\mu f_\mu \rho \frac{k^2}{\epsilon} \tag{3.11}$$

$$P = \tau_{ij}^{turb}\frac{\partial u_i}{\partial x_j} \tag{3.12}$$

$$D = 2\nu\frac{k}{y^2} \text{ or } 2\nu(\frac{\partial\sqrt{k}}{\partial y}) \tag{3.13}$$

ν= Viscosity (m^2/s)

σ_k= Model constant

k= Turbulent kinematic energy

ε= Dissipation rate

f_1=1

f_2= Extra source term

The air circulation is mostly provided by natural ventilation in the buildings and the natural ventilation velocity must be limited by 0.2 m/s for the occupant's thermal comfort (American Society of Heating, Refrigerating and Air- Conditioning Engineers, 2010). Therefore, the natural ventilation has low Reynold number and this turbulence model was selected in the simulation.

Advection Scheme 5

Advection scheme is one of the most important understanding of heat transfer methodology in CFD analysis. It provides manner for the horizontal heat spread in the simulation calculations.

Numerical method is the main factor in CFD simulations. The selected calculation method provides the continuity in the solutions. In the case of this study, advection scheme 5 of CFD software was preferred. Advection scheme 5 uses "Modified Petrov-Galerkin" calculation method. This method provides the natural convection stability and energy balance stability during the analysis (Url-6).

Continuity equations and the Navier-Stokes equations are governing by partial differential equations in the turbulence model calculations. The physical properties of the turbulent flows can be described by using "Navier-Stokes equations" with the consideration of the Reynolds number in the viscous terms (John, 2016).

Addition to the importance of governing equations, the simulation geometry has a significant effect on the analysis and the geometry is separated as two dimensional geometry and three-dimensional geometry. Two-dimensional geometries are more stable than three-dimensional geometries in the simulations. Three-dimensional flow requires different depended variables. Also, boundary conditions becomes complicated and intuitive (Schnipke, 1986). This situation necessitates the mesh

enhancement work in the simulations. As the simulation geometry is three dimensional and the used method is Petrov-Galerkin, mesh enhancement was focused in this study.

4. RESULTS AND DISCUSSION

The boundary conditions, mesh settings were explained in case study section. Based on the obtained data and specifications about energy performance and CFD analyses, results were simulated and discussed in the following section.

4.1 Energy Simulation Results

The energy simulation software presents the design parameters, loads and consumptions for each type of parameter such as cooling, heating and lighting as explained in the above sections. In this study, heating demand of the building was calculated by energy simulation software.

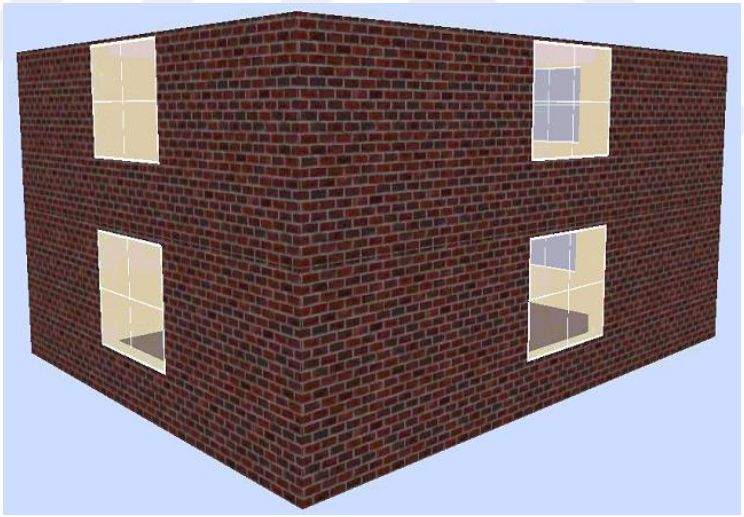

Figure 4.1 : The render view of the building.

The simulation was performed for an entire year and the thermal characteristic of the building elements were defined based on TS-825 standards. The obtained heating demand and the energy consumption of the building was presented in the table below.

Table 4.1 : Energy performance simulation results.

Zone Sensible Heating (kW)	Energy per Building Area (kWh/m^2)
14.87	99.22

The zone sensible heating value presents the size of the heating equipment to meet the zone heat balance. Therefore, the heat generation of the heating equipment must be 14.87 kW at least to provide heating demand.

4.2 Russian Masonry Stove's Performance Simulation Results

4.2.1 Space heating

The temperature results were taken from different eight locations to prove better evaluation. Also, the heat distribution was clearly observed all around the building. The heating process was run for 10 hours based on the working principle of the Russian masonry stove.

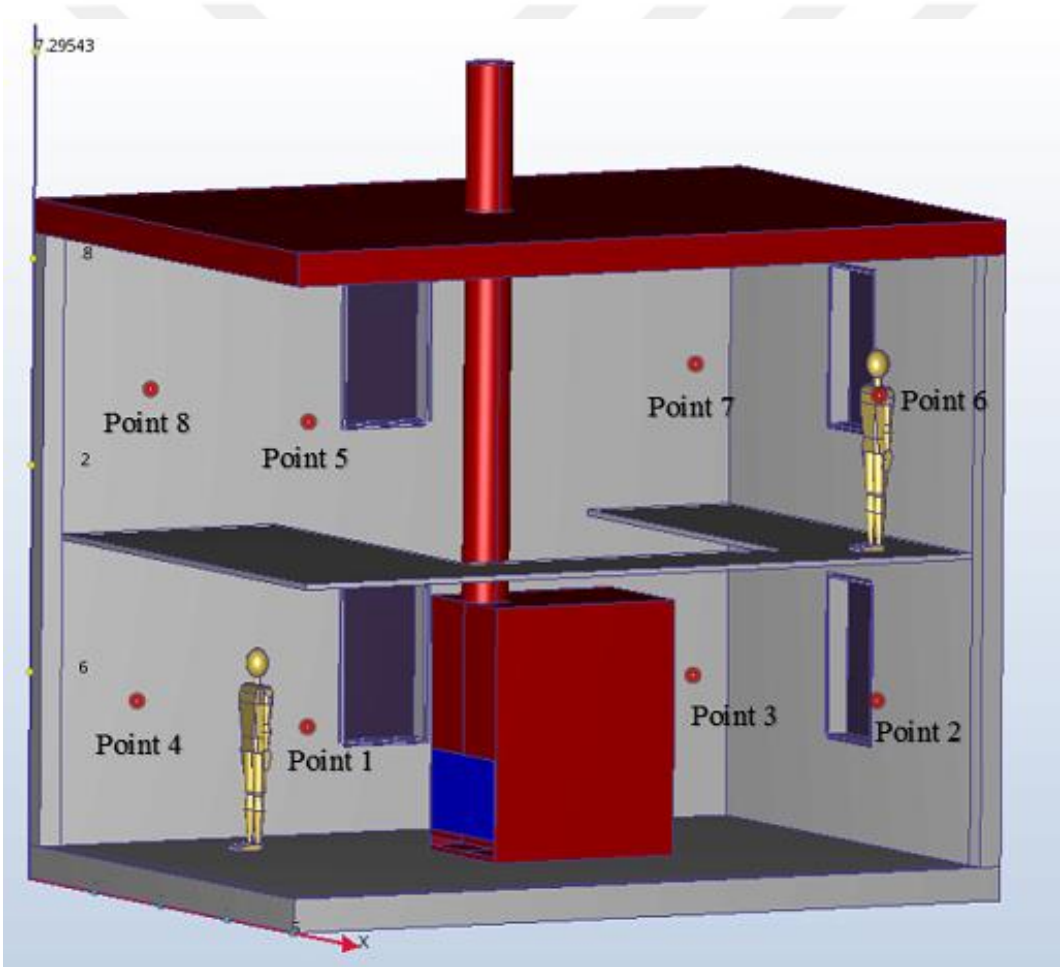

Figure 4.2 : The location of the points in the 3D model.

Four points out of eight points were located on the first floor and the rest of the four points were placed on the second floor. They were situated closer to the corners and the height was defined as 1.4 m from the floor level. Therefore, the temperature change was monitored throughout the building by software.

The simulations repeated till the mesh independency is obtained. In this purpose, the node numbers were increased from 340848 to 827388 while the element number increased from 1344459 to 3448857.

Table 4.2 : Mesh enhancement.

	Element Number	Nodes
Simulation I	1344459	340848
Simulation II	1518968	381576
Simulation III	1875478	476489
Simulation IV	2253507	564957
Simulation V	3448857	827388

Table 4.3 : Temperature data of the simulation I.

Point	Temperature (˚C)
Point 1	29.86
Point 2	28.28
Point 3	28.41
Point 4	27.99
Point 5	29.95
Point 6	28.36
Point 7	28.34
Point 8	27.48

Table 4.4 : Temperature data of the simulation II.

Point	Temperature (˚C)
Point 1	24.00
Point 2	25.09
Point 3	23.78
Point 4	21.99
Point 5	27.48
Point 6	28.34
Point 7	28.41
Point 8	21.29

Table 4.5 : Temperature data of the simulation III.

Point	Temperature (˚C)
Point 1	24.82
Point 2	25.01
Point 3	22.62
Point 4	20.65
Point 5	24.29
Point 6	25.32
Point 7	22.20
Point 8	20.08

Table 4.6 : Temperature data of the simulation IV.

Point	Temperature (˚C)
Point 1	24.15
Point 2	24.55
Point 3	21.65
Point 4	21.33
Point 5	24.68
Point 6	24.08
Point 7	23.69
Point 8	20.28

Table 4.7: Temperature data of the simulation V.

Point	Temperature (˚C)
Point 1	24.82
Point 2	25.40
Point 3	21.11
Point 4	21.45
Point 5	23.99
Point 6	24.90
Point 7	24.79
Point 8	20.28

Temperature distribution was shown with plane section view after 10 hours heating period.

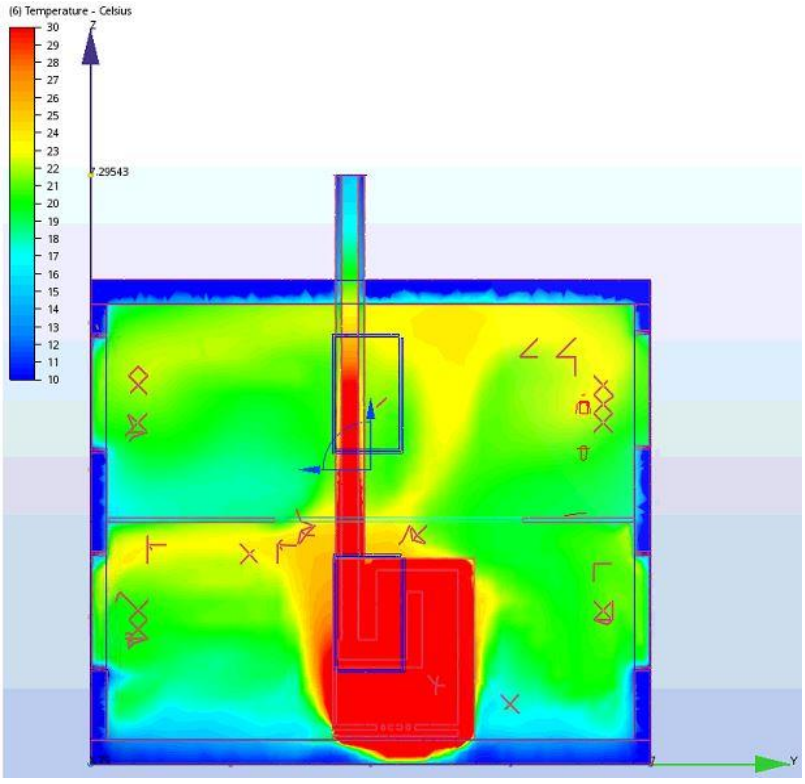

Figure 4.3 : Temperature gradient after heating period.

The results show the temperature difference of the points is around 3%, and Point 6 has a difference like 4.74%. In literature, 5% is the accepted value for the obtainment of mesh independency. Therefore, the mesh improvement was performed till obtaining this range.

Simulation V catches the mesh independency based on the mentioned definition, above. Thus, these results were evaluated to examine thermal comfort and the energy efficiency in this section.

4.2.2 Predicted mean vote

The temperature data shows us how heating capacity of the stove affects the indoor environmental air. In this study, the thermal comfort level was assessed as addition to the energy efficiency of the stove. Hence, PMV results were considered.

The PMV results were obtained by the help of used human figures in the simulations. That human figure is a 3-D model and designed based on real human body size. Also, it can be found in the online library of the 3D modelling software to be used in the studies.

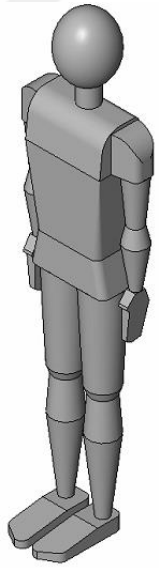

Figure 4.4 : The standing human figure.

These figures are designed based on the real human size. So, observing PMV from the any region of the human becomes available. In this search, that human figure was placed at the both of the first and the second floor and the PMV was assessed for the all floors.

Table 4.8 : Predicted mean vote data after 6 hours heating period.

Location	PMV
1st floor	-0.2
2nd floor	-0.4

The predicted mean vote was visualized by gradient view to obtain proper evaluation.

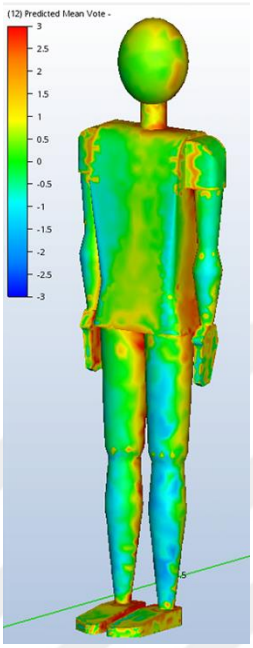

Figure 4.5 : Predicted mean vote view after 6 hours heating period.

The predicted mean vote was evaluated for 10 hours heating period addition to the 6 hours heating period.

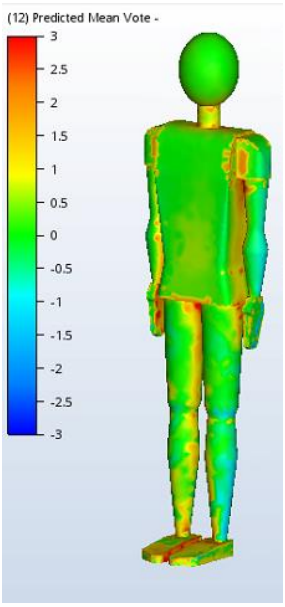

Figure 4.6 : Predicted mean vote view after 10 hours heating period.

Table 4.9 : Predicted mean vote data after 10 hours heating period.

Location	PMV
1st floor	0.3
2nd floor	0.1

The PMV data were examined for 6 hours heating and 10 hour heating, separately. Hence, the influence of the temperature rise regarding to the time was observed within detail.

4.2.3 Standby period

The heating process was stopped after 10 hours. After then, the standby period was observed for 12 hours. In this duration, the temperature data was taken from the mentioned same eight points, identically.

Table 4.10 : Temperature data of the simulation V.

Point	Temperature (˚C)
Point 1	20.72
Point 2	22.26
Point 3	17.15
Point 4	18.05
Point 5	19.84
Point 6	20.64
Point 7	21.45
Point 8	17.89

As explained in the above sections, simulation V results were used based on the mesh enhancement study.

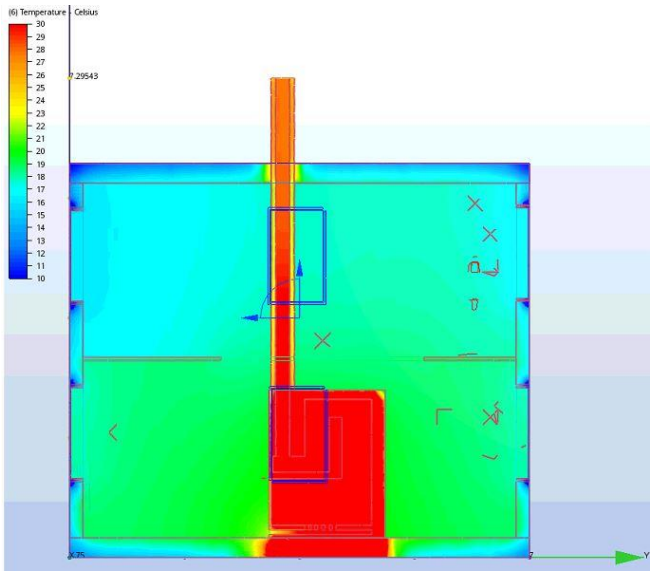

Figure 4.7 : Temperature gradient after standby period.

The predicted mean vote distribution on placed human figures were presented for 6 hours and 12 hours to evaluate the results better.

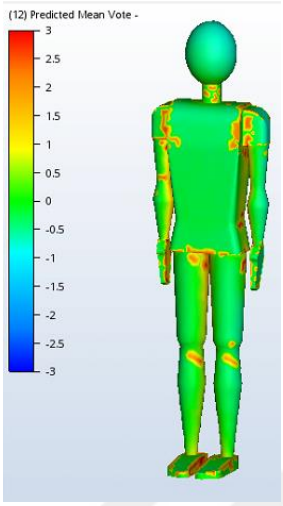

Figure 4.8 : Predicted mean vote view after 6 hours standing period.

The temperature change was observed for 12 hours after completing the heating period. As finalizing 12 hours for standby period, the predicted mean vote data were taken.

Table 4.12 : Predicted mean vote data after 12 hours standing period.

Location	PMV
1st floor	-1.0
2nd floor	-0.7

The visual distribution of predicted mean vote were examined on the human figure after 12 hour standing period, as well.

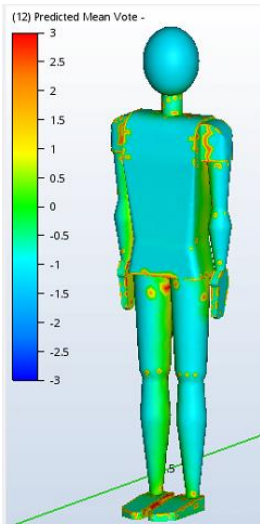

Figure 4.9 : Predicted mean vote view after 12 hours standing period.

4.2.4 Heat flux

The temperature distribution of the building was taken from different points of the building. Besides, PMV values were presented for the floors that the evaluation of the thermal comfort was performed. However, the heat generation amount is important to compare the obtained heat flux to present for heating demand value from energy simulation software.

Heat flux value was taken by using wall calculator option of the CFD software. All of the heat transferred surfaces were selected to obtain results.

Table 4.13 : Heat flux for heating and standby periods.

	Heating Period	Standby Period
Heat Flux (W)	2971	3858

The total heat flux was found as 6829 watts. In energy simulation analysis results, the heating demand of the building was calculated as 14870 watts. The generated heat flux from the stove seems less than the desired level. It should be noted that the heating demand was found by energy simulation software and the calculation conditions differ between the software. However, it is seen that the temperature levels were obtained at the thermal comfort level. Therefore we can understand that even the heat flux amount of the Russian stove seems less, it generates the enough heat output.

4.3 Steel Casting Stove's Performance Simulation Results

4.3.1 Space heating

Steel casting stove simulations were done as a comparison study to Russian stove. In the previous sections, it was explained that these cases differ from each other based on design characteristics and thermal characteristics. The heating period in the steel casting stove was performed for 6 hours.

Table 4.14 : Mesh enhancement.

	Element Number	Nodes
Simulation I	1257844	197658
Simulation II	1545762	356127
Simulation III	1786557	422571
Simulation IV	2049060	585109
Simulation V	2284251	636309

The same heating and standby process were done to evaluate the thermal comfort and energy efficiency of the stoves. The simulations repeated till the mesh independency was obtained.

Table 4.15 : Temperature data of the simulation I.

Point	Temperature (˚C)
Point 1	32.41
Point 2	32.82
Point 3	29.56
Point 4	33.12
Point 5	28.41
Point 6	28.75
Point 7	34.57
Point 8	33.42

Table 4.16 : Temperature data of the simulation II.

Point	Temperature (˚C)
Point 1	26.25
Point 2	26.27
Point 3	26.45
Point 4	28.17
Point 5	26.93
Point 6	25.67
Point 7	28.42
Point 8	27.21

Table 4.17 : Temperature data of the simulation III.

Point	Temperature (˚C)
Point 1	24.58
Point 2	24.60
Point 3	28.36
Point 4	28.48
Point 5	26.74
Point 6	24.94
Point 7	27.41
Point 8	27.14

Table 4.18 : Temperature data of the simulation IV.

Point	Temperature (˚C)
Point 1	22.39
Point 2	22.59
Point 3	28.42
Point 4	28.44
Point 5	21.63
Point 6	23.11
Point 7	30.91
Point 8	28.08

Table 4.19 : Temperature data of the simulation V.

Point	Temperature (˚C)
Point 1	21.50
Point 2	21.40
Point 3	28.42
Point 4	28.44
Point 5	21.63
Point 6	23.11
Point 7	30.91
Point 8	28.08

Based on the given results, mesh independency was obtained in the simulation V and the results of that simulation was used in the examination.

4.3.2 Predicted mean vote

The PMV evaluation was achieved by the placed real human size figures. Therefore, the PMV was examined on the first and second floors, both.

Table 4.20 : Predicted mean vote data after 6 hours heating period.

Location	PMV
1st floor	0.0
2nd floor	2.71

The PMV data were examined for 6 hours heating as the overheating was seen in the temperature distribution. If 10 hours more heating was performed, the PMV would reach 3, as seen clearly**.**

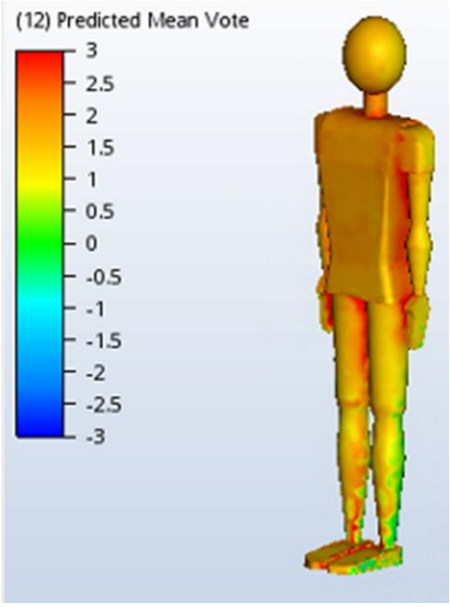

Figure 4.10 : Predicted mean vote view after 6 hours heating period.

4.3.3 Standby period

The heating process was stopped after 6 hours. After then, the standby period was observed for 6 hours more in contrast to 12 hours in Russian stove case. In this duration, the temperature data was obtained from the same eight points. As explained in the above sections, simulation V results were used based on the mesh enhancement study.

Table 4.21 : Temperature data of the simulation V.

Point	Temperature (˚C)
Point 1	16.50
Point 2	16.74
Point 3	19.34
Point 4	19.21
Point 5	16.39
Point 6	17.71
Point 7	19.29
Point 8	19.07

The temperature distribution was shown by thermal gradient for 12 hours standby period.

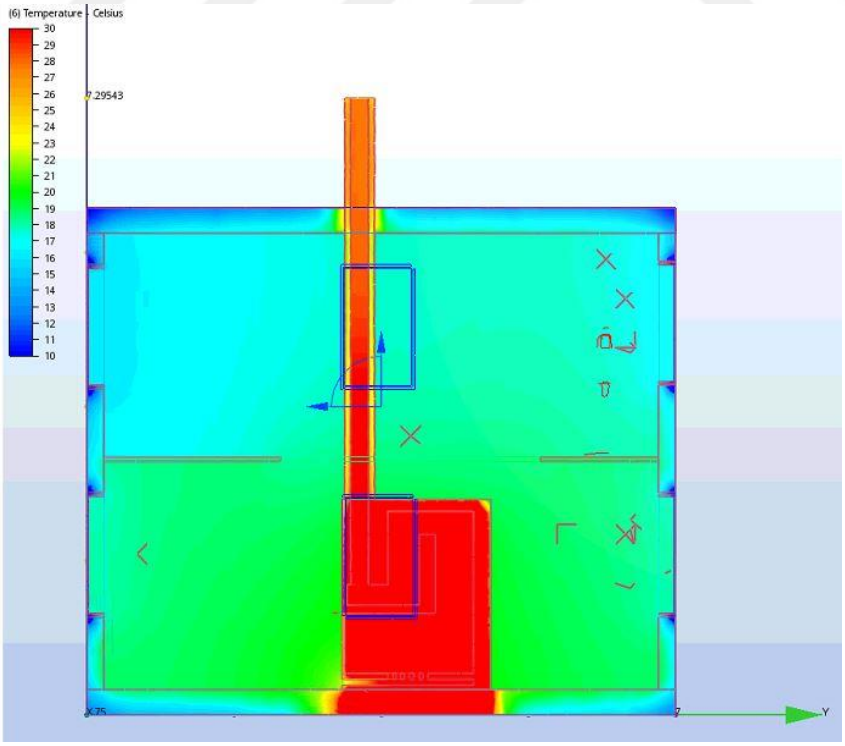

Figure 4.11 : Temperature gradient after standby period.

The effect of thermal gradient was examined better with preicted mean vote data on the human figure.

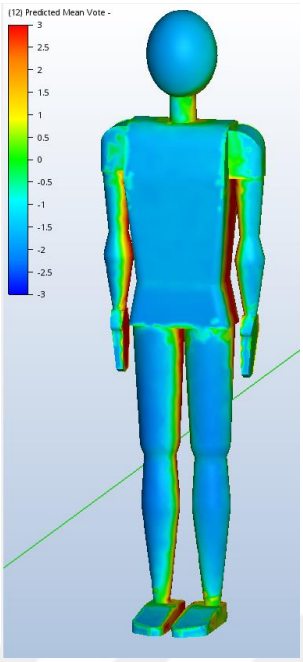

Figure 4.12 : Predicted mean vote view after 6 hours standing period.

Addition to recorded temperature data fluctuating, the PMV data was examined based on 6 hours standby period.

Table 4.22 : Predicted mean vote data after 6 hours standby period.

Location	PMV
1st floor	-1.4
2nd floor	-0.4

4.3.4 Heat flux

In steel casting stove case, the temperature distribution of the building was mentioned for different points of the building as in the case of Russian stove PMV values were obtained to evaluate the thermal comfort. The heat generation amount is important to compare the obtained heat flux values to present for heating demand value from energy simulation analysis. Heat flux values were taken from all of the heat transferred surfaces.

Table 4.23 : Heat flux for heating and standby periods.

	Heating Period	Standby Period
Heat Flux (W)	4075	1227

The total heat flux was found as 5302 watts. In energy simulation results, the heating demand of the building was calculated as 14870 watts.

4.4 Velocity Results

In the analysis of heating period, the air movement has a significant importance. If the velocity is faster or slower than defined range, as explained in the previous sections, it affects the thermal comfort, negatively. Addition to this, the air velocity is needed to be observed to see if there is a backward movement inside the stove. Therefore, the velocity was examined for velocity magnitude and z direction velocity magnitude, separately.

The air circulation velocity should be less than 0.2 m/s to provide thermal comfort conditions in the building. In Russian stove case, it is seen that the velocity magnitude increases around the stove based on hot air movement. However, the air velocity magnitude was found around 0.1 m/s, generally.

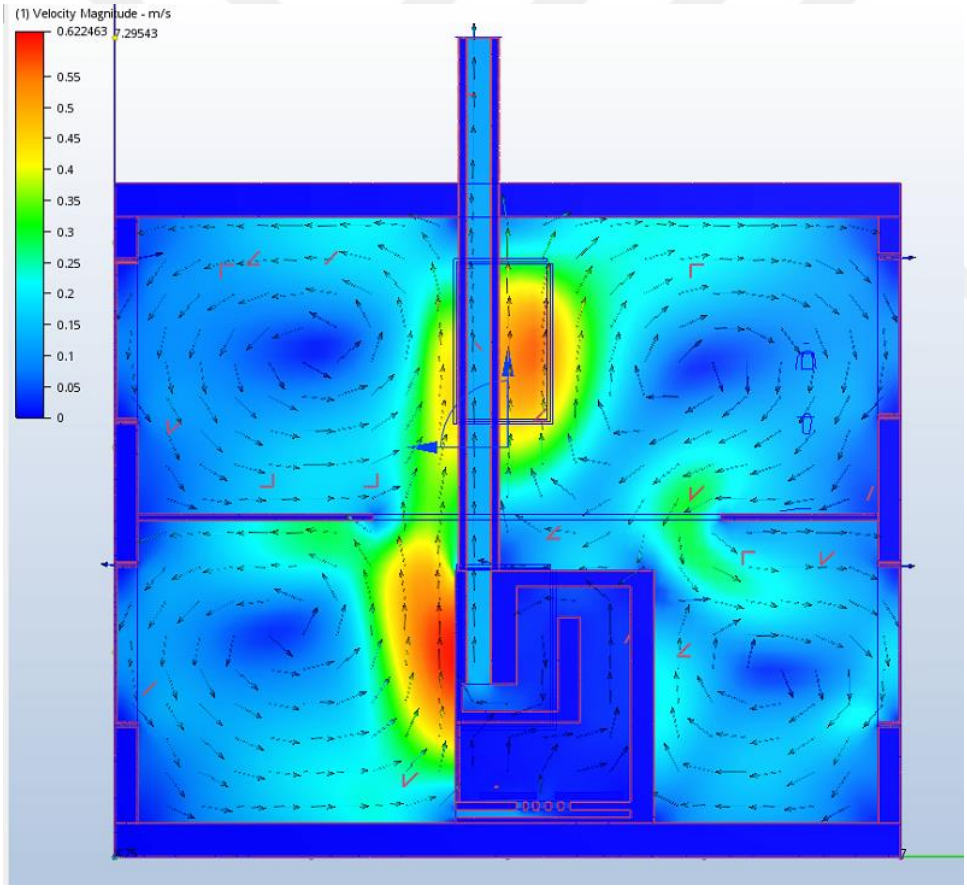

Figure 4.13 : Air circulation by a section view for Russian stove case.

Velocity magnitude is helpful to evaluate the thermal comfort. On the other hand, z direction velocity should be considered to find out the backward movement in the chimney. In the case of Russian stove, the z direction velocity is in regular form without causing any backwards circulation.

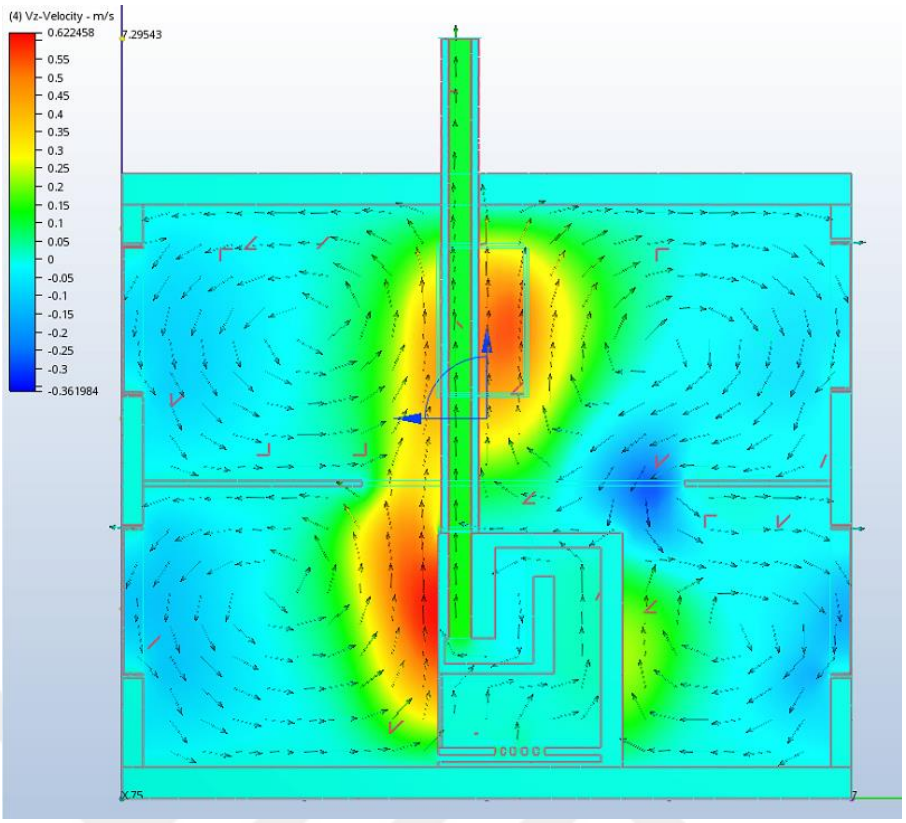

Figure 4.14 : Z direction air velocity circulation by a section view for Russian stove.

Velocity magnitude and z direction velocity value were examined for steel casting stove, as well. The velocity magnitude kept less than 0.2 m/s as intended in the beginning of the study.

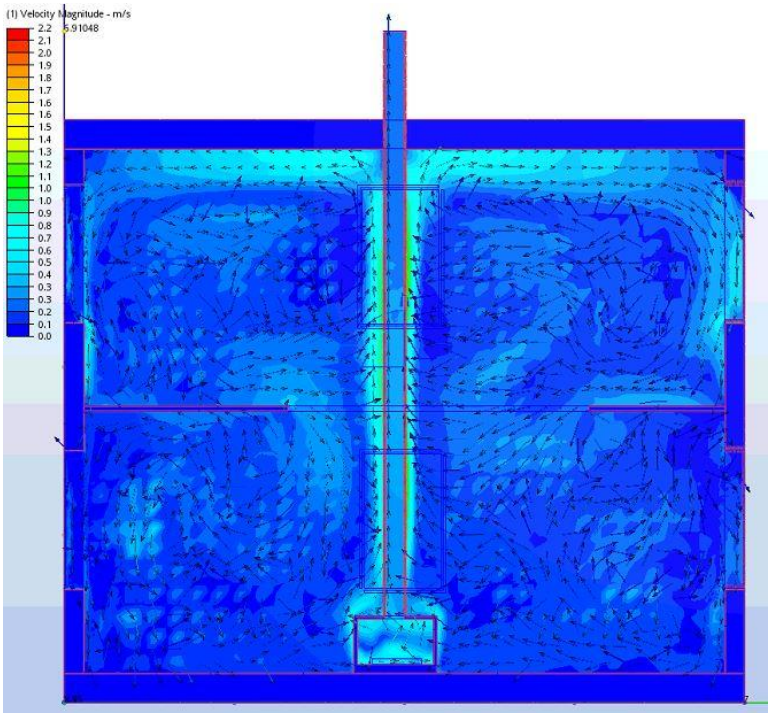

Figure 4.15: Air velocity magnitude for steel casting stove case.

Z direction velocity value shows that the smoke movement is faster than Russian stove case in the chimney. Additionally, no backwards movement occurred. Therefore, indoor air quality is protected.

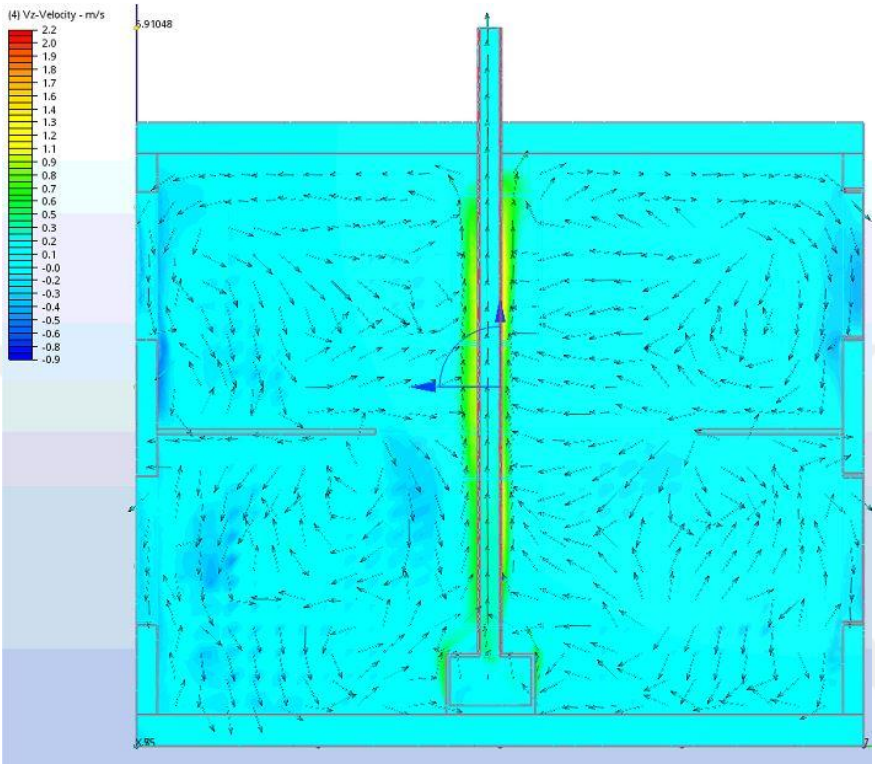

Figure 4.16 : Z direction air velocity circulation by a section view steel casting stove case.

4.5 Comparison of the Results

The results were given for the both examined cases. The results were obtained by mesh enhancements and these simulations were evaluated in the conclusion as mentioned above. To summarize the results from point 1 (1st floor) and results from point 3 (2nd floor) were given in the tables below.

Table 4.24 : Temperature data on the point 1 and point 3 for Russian stove.

	Russian Stove (Point 1)	Russian Stove (Point 3)
Temperature after heating period (˚C)	24.82	24.79
Temperature after standby period (˚C)	20.72	21.45

Table 4.25 : Temperature data on the point 1 and point 3 for steel casting stove.

	Steel Casting Stove (Point 1)	Steel Casting Stove (Point 3)
Temperature after heating period (˚C)	21.50	29.87
Temperature after standby period (˚C)	16.50	19.29

Table 4.26 : Predicted mean vote on the 1st floor and the 2nd floor for Russian stove.

	Russian Stove (1st floor)	Russian Stove (2nd floor)
PMV after heating period (˚C)	0.3	0.1
PMV after standby period (˚C)	-0.35	-0.15

Table 4.27 : Predicted mean vote on the 1st floor and the 2nd floor for steel casting stove.

	Steel Casting Stove (1st floor)	Steel Casting Stove (2nd floor)
PMV after heating period (˚C)	0.0	2.71
PMV after standby period (˚C)	-1.4	-0.4

Table 4.28 : The heat flux results of the examined cases.

	Russian Stove (Point 1)	Russian Stove (Point 3)
Heat Flux (W)	6829	5302

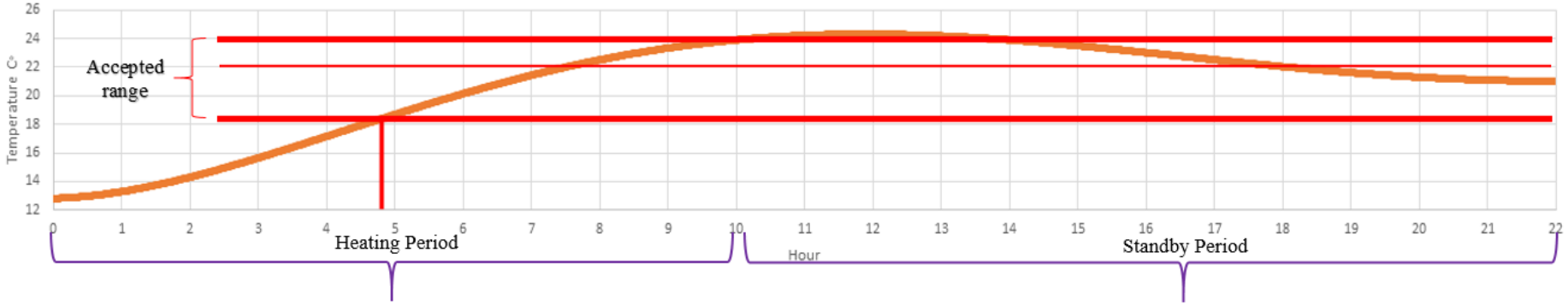

Figure 4.17 : Temperature-time graph for Russian stove.

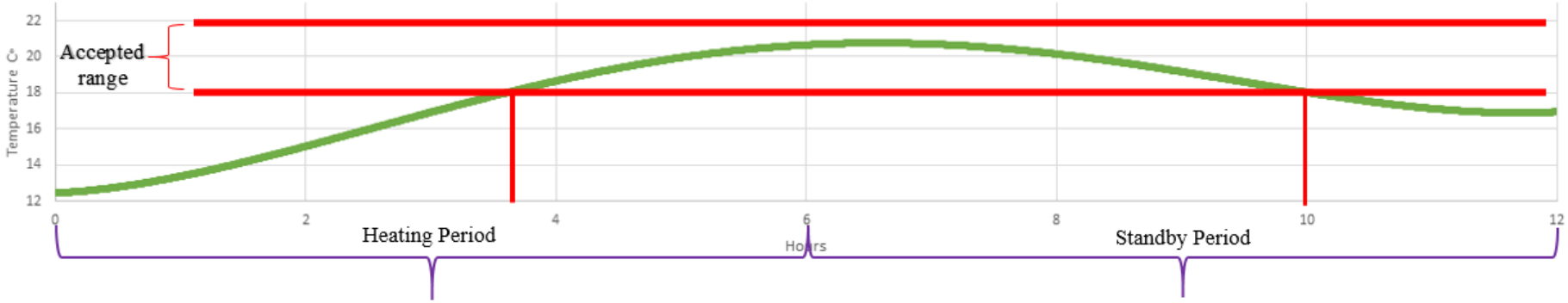

Figure 4.18: Temperatur**e**-time graph for steel casting stove.

The temperature vs time graphics were created for both cases. These graphs show when the thermal comfort temperature was obtained in the heating period. In these graphics, the temperature data of point 1 was taken. Also, they present how temperatures change during the standby period.

In the case of Russian stove, 18˚C was obtained on the fifth hour of the heating period. The heating period was finalized after 10 hours, however, temperature continued to rise for 1 hour more. This situation caused based on the firestone material specification. After heating period, standby period was simulated for 12 hours. In this period, it was seen that the generated temperature was protected.

In the case of steel casting stove, 18˚C was caught after 4.5 hours in the heating period. The heating period was finalized after 6 hours. Maximum temperature was found as 21.5˚C. After heating period, the standby period was simulated for 6 hours. In this period, it was seen that the temperature reduced from 21.5˚C to 18˚C in 4 hours. When 6 hours standby period was finalized, the temperature was 16˚C, nearly.

5. CONCLUSION

Steel casting stove and Russian stove were compared based on their eergy performance and heat flow. The generated heat flow were evaluated by CFD analysis while the energy performance was assessed by taking the advantage of energy simulation software.

The study was carried out for heating and standby periods, separately. The duration of the heating was for 10 hours for Russian stove while the standby period was simulated for 12 hours. In the case of steel casting stove, the heating period was simulated for 6 hours while the standby period was simulated for 6 hours.

The temperature data were monitored at eight different points in the case building by the software. The four points out of eight points were located in the first floor while the other four points were placed at the second floor of the building. Addition to the monitoring points, the human figures were placed at the first floor and second floor to see the PMV in the house.

In the heating and standby period, the heat flux values were recorded to evaluate the heat output from the stoves. Hence, satisfactory circumstances were created to evaluate the thermal comfort.

The mesh enhancement study was performed to obtain the correct results in the CFD simulations and the mesh enhancement was repeated until the difference of the results were reduced to 5%.

In the energy simulations results, the heating demand of the building was found as 14.87 kW which means the heat generation of the stove must be minimum 14.87 kW to cover the heating demand of the building.

In the case of steel casting stove, the indoor temperature was increased very fast and heterogeneous temperature distribution was observed during the heating period. The temperature was found around 20°C-27°C. In the standby period, the temperature dropped very quickly as the increment in the heating period.

PMV value was found as 2.71 in the heating period which is high when considering thermal comfort evaluation.

In Russian stove case, the indoor temperature went up very slowly during 10 hours and the desired temperature levels of 22°C-24°C were obtained after 8 hours. The standby period was simulated for 12 hours and it was observed that the indoor temperature was conserved and the temperature reduced to 18°C-19°C after 12 hours.

In the heating period, PMV was found between 0.3~0.1 while it was between -1~-0.7 in the standby period.

The heat flux data was taken from the all surfaces of the stoves. The heat flux was found as 6829 and 5302 watts for Russian stove and steel casting stove, respectively. The heating demand of the building was calculated as 14.87 kW by energy simulation software.

The monitored temperature data by CFD, PMV values and heat flux amounts present the thermal conditions were obtained in the case of Russian stove. The material specifications, the S-shaped chimney design and the size of Russian stove are the main parameters on the achievement of thermal comfort levels.

This study specifies that the collaboration work of the various disciplines such as architectural, material science and the mechanical engineering created a good example for an energy efficient heating system and this system was examined CFD analysis. For future works, the integration of this system to the apartment building that has multiple residential units can be investigated by a detailed study.

REFERENCES

ANSI/ASHRAE Standard 55. (2010). Thermal Environmental Conditions for Human Occupancy, *ASHRAE*, Atlanta, GA . https://doi.org/ISSN 1041-2336

Bardina, J. E., Huang, P. G., & Coakley, T. J. (1997). Turbulence Modeling Validation, Testing, and Development. *Nasa Technical Memorandum, (110446)*, 8–20. https://doi.org/10.2514/6.1997-2121

Canada Mortgage and Housing Corporation. (2002). A guide to Residential Wood Heating

Cardarelli, F. (2008). Ceramics, Refractories, and Glasses. *Materials Handbook: A Concise Desktop Reference*, 593–689. https://doi.org/10.1007/978-1-84628-669-8

European Commision. (2014). A policy framework for climate and energy in the period from 2020 to 2030, Brussels. https://doi.org/10.1007/s13398-014-0173-7.2

European Energy Agency. (2015). Final energy consumption by sector and fuel. Indicator Assessment Data and Maps, 20. https://doi.org/CSI 027/ENER 016

Eurostat. (2012). In the EU27, Almost half of renewable energy comes from wood & wood waste, (November). https://doi.org/168/2012

Eurostat. (2013). Manual for statistics on energy consumption in households. https://doi.org/10.2785/45686

Feist, W., Schnieders, J., Dorer, V., & Haas, A. (2005). Re-inventing air heating: Convenient and comfortable within the frame of the Passive House concept. *Energy and Buildings*, *37*, 1186–1203. https://doi.org/10.1016/j.enbuild.2005.06.020

Georges, L., Skreiberg, Y., & Novakovic, V. (2013). On the proper integration of wood stoves in passive houses: Investigation using detailed dynamic simulations. *Energy and Buildings*, *59*, 203–213.

Georges, L., Skreiberg, Y., & Novakovic, V. (2014). On the proper integration of wood stoves in passive houses under cold climates. *Energy and Buildings*, *72*, 87–95. https://doi.org/10.1016/j.enbuild.2013.12.023

Grondzik, W. T., Kwok, A. G., Stein, B., & Reynolds, J. S. (2010). Mechanical and Electrical Equipment for Buildings

Hanley, P. M., Saez, D., Nielson, C., & Warneck, H. (2005). Efficiency Study of a Contraflow Masonry Wood - Burning Heater.

Incropera, F. P., DeWitt, D. P., Bergman, T. L., & Lavine, A. S. (2007a). Fundamentals of Heat and Mass Transfer. https://doi.org/10.1073/pnas.0703993104

Incropera, F. P., DeWitt, D. P., Bergman, T. L., & Lavine, A. S. (2007b). Fundamentals of Heat and Mass Transfer. https://doi.org/10.1073/pnas.0703993104

Jagadeesh, P., & Murali, K. (2005). Application of Low-Re Turbulence Models for Flow Simulations Past Underwater Vehicle Hull Forms. *Journal of Nacal Architecture and Matine Engineering, 1*, 42-54

Kajishima, T., & Taira, K. (2017). Computational Fluid Dynamics. https://doi.org/10.1007/978-3-319-45304-0

Organization for Economic Cooperation and Development. (2012). World Energy Outlook 2012

Recktenwald, G. (2009). The k−∈ Turbulence Model, 1–20. Retrieved from http://web.cecs.pdx.edu/~gerry/class/ME448/notes/pdf/keModel.pdf

Schnipke, R. J. (1986). A streamline upwind finite element method for laminar and turbulent flow. Retrieved from http://www.omnitech.co.il/UserFiles/File/Benny/Schnipke_PhD.pdf

Scott-Pomerantz, C. D. (2004). The K-Epsilon Model in the Theory of Turbulence. *Thesis*, 59.

Sturc, M. (2012). Renewable energy - Analysis of the latest data on energy from renewable sources. Eurostat - Statistic in Focus, 1–8.

TS 825. (2013). Thermal Insulation Rules in Buildings, *Turkish Standardization Institute*, Ankara

U.S. Department of Energy. (2008). Energy Efficiency Trends in Residential and Commercial Buildings. *Energy*, 1–32.

Url-1<http://ec.europa.eu >, date retrieved 25.04.2018.

Url-2 <https://www.energydepot.com>, date retrieved 25.04.2018.

Url-3<http://krisdedecker.typepad.com>, date retrieved 25.04.2018.

Url-4 <https://www.designbuilder.co.uk>, date retrieved 25.04.2018.

Url-5 < http://help.autodesk.com>, date retrieved 25.04.2018.

Url-6 < https://knowledge.sutodesk.com>, date retrieved 25.04.2018.

Url-7 <https://www.cfd-online.com>, date retrieved 25.04.2018.

CURRICULUM VITAE

Name Surname : Hale Tuğçin KIRANT

Place and Date of Birth : Istanbul / 1990

E-Mail : kiranth@itu.edu.tr

EDUCATION:

B.Sc. : 2015, Marmara University, Engineering Faculty, Mechanical Engineering

PROFESSIONAL EXPERIENCE AND REWARDS:

- Istanbul Technical University-Energy Institute- Research Assistant, 2017-Cont.
- FP7-R2CITIES Project- Researcher, 2017-Cont.
- FP7-CITYFIED Project- Researcher, 2016-Cont.

PUBLICATIONS, PRESENTATIONS AND PATENTS ON THE THESIS:

▪ Kırant H. T**.,** Sözer H., 2018: Comparative Analysis of Traditional Masonry Chimneys through Energy Performance and CFD Analyses to Assess the Indoor Comfort Conditions. *International Congress - 3rd Sustainable Development of Energy Water and Environment Systems*, June 29- July 04, 2018 Novi Sad, Serbia.

▪ Kırant H. T**.,** Sözer H., 2018: Comparative Analysis of Traditional and Contemporary Stoves Based on Their Energy Performance. *International Congress – 7th International Congress on Current Debates in Social Sciences*, April 19-20, 2018 Istanbul, Turkey.

OTHER PUBLICATIONS, PRESENTATIONS AND PATENTS :

▪ Sözer H., Kırant H. T., 2018: Comparison of the Waste District Heating System with Conventional Heating Systems Based on their Energy Performance. *International Conference – Energy Systems Conference 2018*, June 19-20, 2018 London, UK.

▪ Sınar Ü., Kırant H. T., Mançuhan E., Yılmaz B., Sevindir M. K., 2016: Energy and Cost Analysis of the Alternative HVAC System Applications for a College Building in Doha Qatar. *International Conference – 12th International HVAC+R & Sanitary Technology Symposium,* 31 March-02 April 2016 İstanbul, Turkey.